THESIS

MODELLING THE EFFECTIVE PROPERTIES OF MAGNETO-ELECTRO-ELASTIC THREE-DIMENSIONAL CELLULAR SOLIDS

Submitted by

Sandhya Kannan

Department of Civil and Environmental Engineering

In partial fulfillment of the requirements

For the Degree of Master of Science

Colorado State University

Fort Collins, Colorado

Spring 2020

Master's Committee:

Advisor: Dr Paul Heyliger

Suren Chen
Christian Puttlitz

ABSTRACT

MODELLING THE EFFECTIVE PROPERTIES OF MAGNETO-ELECTRO-ELASTIC THREE-DIMENSIONAL CELLULAR SOLIDS

Cellular solid foams are increasingly used in various industries right from disposable coffee cups to crash padding of an aircraft cockpit. Hence it is important to understand the structure and properties of cellular solids and the ways their properties can be utilized in engineering design. Using the method of Finite Element analysis three-dimensional cellular solids made up of Magneto-Electro-Elastic (MEE) materials were studied. A FORTRAN code was written to implement the models in order to determine the effective mechanical properties for the solid under study. Computational model was created and properties such as elastic, piezoelectric and piezomagnetic and permittivity were studied as a function of relative density. Result obtained for purely elastic properties were plotted against the relative density. Different thickness of the three-dimensional foam under consideration was studied by varying the Poisson's ratio. The obtained results of the jack packed cellular foam analysis gave a similar behavior of other foam structures thus verifying the accuracy of the model.

ACKNOWLEDGEMENTS

I would first like to thank my thesis advisor Dr. Paul Heyliger, the door to his office was always open whenever I ran into trouble or had as question about my research or writing. He steered me in the right direction whenever he thought I needed it.

I also thank the Supreme Lord who gave me the strength, health and ability to finish the thesis.

Finally, I must express my very profound gratitude to my mother, grandparents and to my friends for providing me with unfailing support and continuous encouragement throughout my years of study and through the process of researching and writing this thesis. This accomplishment would not have been possible without them.

DEDICATION

Dedicating my thesis to Mr and Mrs ThillaiNayagam

TABLE OF CONTENTS

LIST OF FIGURES

CHAPTER 1

INTRODUCTION

1.1 MOTIVATION

The structure of the cells captivated researchers for at least 300 years. Cellular solids commonly referred as clusters of cells is obtained by arranging each unit cells with solid faces or edges packed together so that air fills the volume of space between the cell walls. Naturally occurring cellular solids such as wood, cork, coral, sponge is used by man for thousands of years. In recent years artificial cellular solids are manufactured from materials like polymers, ceramics, metals and glasses to yield the desired qualities. The shape of these vary from even shapes to a more random configuration. In many studies of cellular solids, the results are not always in agreement. Hence a more precise and resourceful research is required in this topic.

Based on the cell walls the foams can be categorized as open, closed or partially closed structures. Examples of foam categories are shown if figure 1.1. The left most figure shows the honeycomb pattern cell shape and the center, and the right figure represents the three dimensional open and closed cell foam. These foams have a widespread industrial application in fields like nuclear industry, superconducting sensors, electronics industry, impact absorbers and light weight sandwich panels.

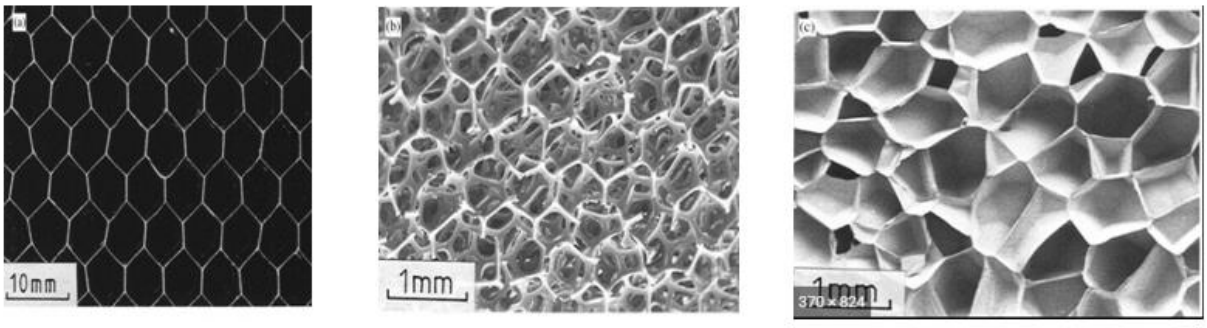

Figure 1.1: Two-dimensional honeycomb, Three-dimensional open cell foam, Three-dimensional closed cell foam. (Gibson and Ashby, 1989).

In Figure 1.2, examples for naturally occurring cellular solids with different cell shapes are shown. In this research three dimensional cellular foams that are composed of MEE constituents are considered and their effective properties is determined. A FORTRAN code using finite element approximation is used to determine the effect of cell shape and the relative density on the properties of the foams.

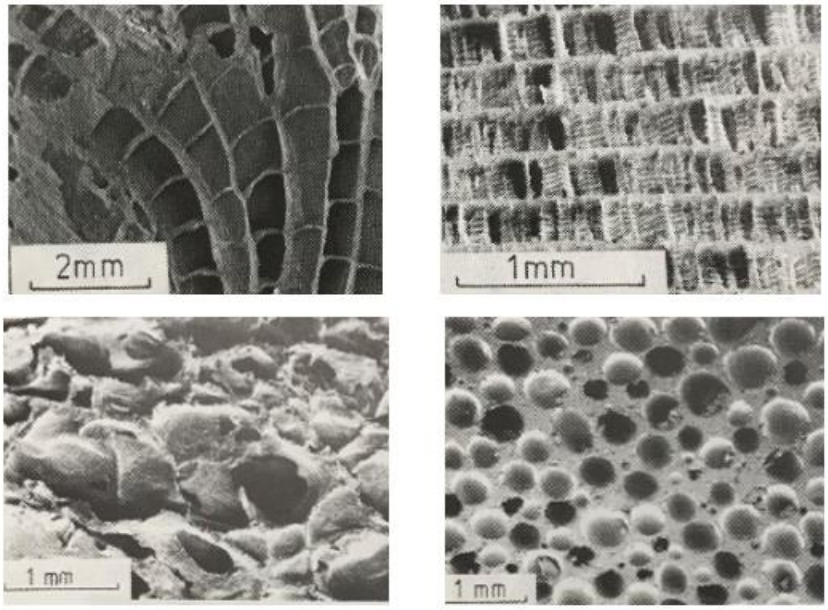

Figure 1.2: Cellular solids in nature: (A) Cancellous bone (B) Coral (C) Bread (D) Chocolate bar

1.2 OBJECTIVES

The primary goal of this thesis is to find the effective properties of three-dimensional cellular foams made of piezoelectric and piezomagnetic material. This goal is expanded into several key objectives as follows:

1. Develop a computational model using finite element approximations for the cellular foams.
2. Determine the effective elastic properties for the jack packed foam structure at varying t/l ratio.
3. Determine the effect of varying cell edge thickness on these effective properties.
4. Study the effect of relative density of foams on all the properties.
5. Determine the effective piezoelectric and piezomagnetic properties of foams at various boundary conditions.

1.3 STRUCTURE OF THE REPORT

The entire thesis is divided into five chapters. The current chapter is Chapter 1 which gives the introduction about the topic and explains the need for the present study. Chapter 2 presents the literature review which gives a deeper understanding of the cellular solids from pervious researches. It gives the overview of magneto electric effect followed by the numerical and analytical modelling of cellular foams. Chapter 3 is divided into 5 sections. The cell structure and configuration are explained in first section followed by the governing equations in the second section. The boundary conditions used are described in section 3 along with the theory for affine motion and the weak form is derived in section 4. The final section explains how each parameter are used to calculate the constant. Once these methods are explained the results and discussions are presented in Chapter 4. Comparison between the present research and the previous studies are tabulated wherever applicable. Discussions on the results is also explained in this Chapter. The final chapter discuss the conclusions derived from the research and suggests any possible future

work that can be done to further and improve this study. An appendix is included which provides the element matrix equations in the Ritz-based model for the coefficient matrices.

CHAPTER 2

LITERATURE REVIEW

This chapter comprises a review of studies related to the present study. The chapter is organized in such a way that background information is presented first followed by the descriptions and conclusions of the research. Reviews on numerical, analytical models and magneto electro effect on foams are included along with other smart materials.

2.1 BACKGROUND

Most of the background information on Cellular Solids was taken from the book Cellular Solids Structure and Properties (1997), by Gibson and Ashby. The cellular solids can be of either two dimensional commonly referred as honeycombs or of three dimensional known as cellular foams. Significant works has been done in attempts to accurately find the properties and behavior of these cellular solids.

Our focus is on three dimensional cellular foams. Understanding the geometry of these foams has a lineage almost different from that of honeycombs. For many years, it has been assumed that the space filling the cells for a minimized surface area per unit volume was by Kelvin's tetrakaidekahedron with slightly curved faces (Kelvin, 1887). Nevertheless, recent computational study by (Brakke, 1992 and Phelan, 1994) shows that a lower surface area per unit volume by about 0.3% can be achieved. The unit cell used by Kelvin is shown in figure 2.1 (A). 2.1 (B) shows the unit cell studied by Phelan. It can be seen that cell has six 14-sided polyhedral and two 12-sided polyhedral cell shape.

Figure 2.1: (A) Kelvins tetrakaidekahedral cell (B) Brakke and Phelan's unit cell

2.2 CLASSIFICATION OF FOAMS

These foams can be either open cell or closed cell. If the cell edges consist all the solid material, then it is identified as an open cell foam. These are formed by the bursting of the membranes which separates individual cells and can be perfected as a random assortment of struts. If the membranes remain intact with most of the solid material in the edge it is known as closed cell foam. These foams have a wide variety of cell shapes and the following figure 2.2 shows the most possible shapes packed together to fill the space.

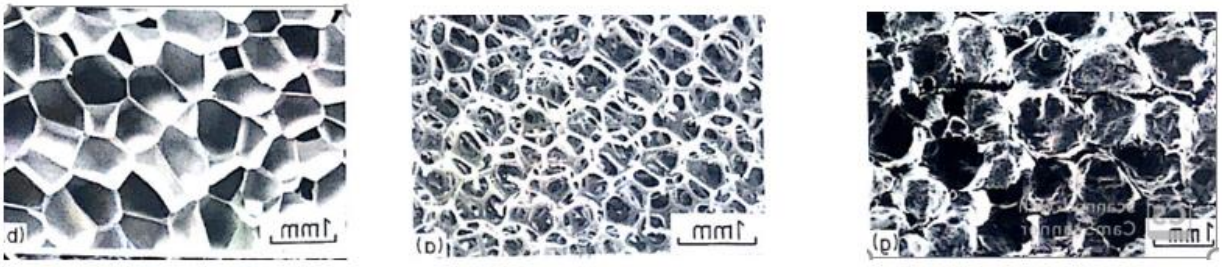

Figure 2.2: Three-dimensional foam materials (A) Open cell polyurethane (B) Closed cell polyethylene (C) Polyether foam with both closed and open cells. (Gibson and Ashby, 1989).

Of all the properties the relative density is the most important trait of the foam. Except Poisson's ratio, most of the elastic constant are directly proportional to this relative density. These constants can be related to its relative density by using the following relation.

$$\frac{\emptyset^*}{\emptyset_s} = c\left(\frac{\rho^*}{\rho_s}\right)^p \quad (2.1)$$

Where:

$\emptyset^*$ is the mechanical property of the foam,

$\emptyset_s$ is the mechanical property of the corresponding solid being considered,

$\frac{\rho^*}{\rho_s}$ is the relative density

P and c are the constants which depend on the foam microstructure

The present study deals predominantly with the modelling the of three-dimensional cellular foams constituted of materials that couple electric and magnetic fields along with elastic properties.

2.3 MAGNETO ELECTRO EFFECT

Sun and Kim (2000) were the first to propose MEE composites. They found a way to get maximized conversion of energy (mechanical) into electric or magnetic by developing a systematic design of MEE composites. The materials used are piezoelectric barium titanite (BaTiO3) and piezomagnetic cobalt iron oxide (CoFe2O4). Out of this BaTiO3 is embedded into the matrix of CoFe2O4. Fully coupled MEE theory is used to find how the energy is converted. Solid isotropic material with penalization (SIMP) and micromechanics model are used as a device for topology optimization. However, using SIMP deriving distinct states of piezoelectric and piezomagnetic is found to be tough. Due to material interactions in the composite the strain will disturb the piezomagnetic phase inducing a magnetic field. The same pattern can be observed while applying electric field instead of magnetic field.

Pan (2001) was the first to develop a 3D exact solution for simply supported plate made of either piezo electric or piezomagnetic materials. This made the homogenization so simple and it resembles the Stroh formalism. They used Piezoelectric BaTio3 and magneto strictive CoFe2O4

for the experiment. Under the application of static surface and internal stresses they found the exact solution for displacements, stress, electric and magnetic potential. Their results also showed that the above physical parameters are influenced by the stacking sequences of the sandwiched materials. Zheng Zhong, Xu Wang (2003) also derived the exact solution but they did the experiment on MEE cylindrical shell and obtained the solution based on Pseudo-Stroh formalism.

Pan and Heyliger (2002) extended the static solution developed by Pan (2001). They found the exact analytical solution for anisotropic 3D MEE plate with all its edges in simply supported condition. They found that when the modes are purely elastic, they will not produce any potentials. On the other case for the coupling modes the electric and magnetic potentials depends upon the magnetic properties and stacking sequences. They found the exact solution by using a propagator matrix and a simple formalism resembling to Stroh formalism.

Ramirez et al (2006) established an approximate method for elastic displacements, electric potential and magnetic potential of a 2D MEE laminate by the combination of discrete layer method with Ritz method. Using ABACUS, they then validated the results by comparing it with exact solution and with FE analysis.

Harshe et al. (1993) created a model for magnetoelectric composites. They were the first to create a working model of MEE foams. (0-3) represents that one of the materials is in particles form representing 0 and the other material is continuous in all the three directions and vice versa for 3-0. They compared their results with the already existing work.

Van Run et al. (1974) found the magnetoelectric effect by coupling the piezomagnetic spinel cobalt ferrite-cobalt titanate with barium titanate which is a piezomagnetic perovskite. The effect was obtained due to the mechanical coupling between the composites. The magnetoelectric

effect is the product between the piezoelectric charge generation q/S and piezomagnetic deformation S/H.

For the last two decades, more researchers have interest on the ME coupling and several works has been carried out in this field.

Smittakorn and Heyliger (2000) modelled a 3D discrete-layer and developed it to study the steady state and transient behavior of the laminated hygrothermo piezoelectric plates under numerous boundary conditions. The problem is done by using simple matrix and solved by using Newmark beta method. The laminates are excited for its surface traction, electric potential, temperature and moisture concentration on all the sides of the laminate.

Aboudi (2001) deliberate the thermomechanical, electric and magnetic fields of sensitive composites that are modelled through homogenization using the fully coupled electro-magneto-thermos elastic (1-3) constitutive laws and compared with generalized method of cells and the Mori-Tanaka predictions. He conducted the experiment on BaTiO3 and CoFe2O4. The results matched and can be used to analyze other effects as well.

Nan (1994) considered the stress distribution of composites due to thermal expansion. Composites such as BaTiO3 which are made from piezoelectric and non-piezoelectric phases are considered. Figure 2.3 shows the MEE composites used in this study. When these materials are subjected to uniform temperature change, an electric polarization is caused because of the mismatch in thermal expansion coefficients. This concept of piezoelectric and thermal expansion is called secondary pyroelectricity. He conducted it mainly to get the product property of two non -pyroelectric materials.

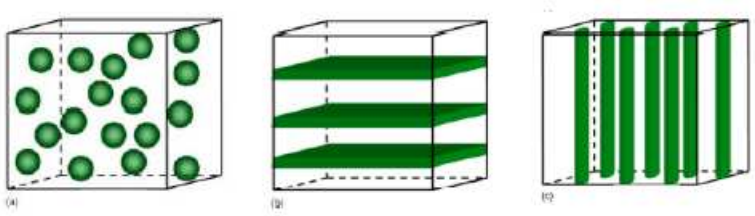

Figure 2.3: MEE Composites types (A) (0-3) particulate composite, (B) (2-2) Laminate composites (C) (1-3) Fibrous composites.

Akbarzadeh and Pasini (2013) studied the effects in cylinders. They studied the outcome among moisture, temperature, magnetic, electric and elastic fields when they are mingled physically on functionally graded cylinder, which is infinitely long and axisymmetric using hygro-thermo-magneto-electro-elasticity theory. To do this they decoupled the governing equation first and then imposed the boundary and interfacial conditions which is either perfect or imperfect. Exact solution for each layers of the cylinder was found.

Zhang and Wang (2015) examined the multi field properties of electro magneto thermoelastic composites (1-3) along with the pyroelectric and pyro-magnetic effects. The multifield of the smart composites were obtained numerically by means of homogenization. The distribution of displacement electric and magnetic potential in RVE at a uniform temp is calculated and compared with Mori Tanaka method. The results showed that the cross-section shape of the enclosure fiber has influence on the in plane thermal related properties of the composite.

2.4 MODELLING OF ISOTROPIC CELLULAR FOAMS

2.4.1 ANALYTICAL MODELS

Gibson and Ashby (1982) modelled the cubic cell where the cell structures are staggered. By doing this, the midpoint of the horizontal edge will be in attachment to the vertical edge. They observed the deformed foam using a microscope and figured that the bending was the main cause for linear elastic deformation in low density foam. They designed their model in such a way that all the edges have a square cross section.

They found the Poisson's ratio equal to 0.33 and developed the following equation.

$$\frac{E^*}{E_S} = C_1 \left(\frac{\rho^*}{\rho_s}\right)^2 \tag{2.2}$$

$$\frac{G^*}{E_S} = C_2 \left(\frac{\rho^*}{\rho_s}\right)^2 \tag{2.3}$$

Where E* is the elastic modulus, Es is the elastic modulus of foamed materials and G* is the shear modulus. The values of C1 and C2 are found from experimental data as 1.0 and 0.4 respectively. Due to low relative densities ($\frac{\rho^*}{\rho_s} \leq 0.1$), the effect of shear and axial deformation were neglected in the model.

Menges and Knipschild (1975, 1982) provided an equation as a function of foam density for their mechanical behavior by studying a rigid Polyurethane foams. They did the experiment using a pentagonal dodecahedral cell. They assumed the cell edge to be a triangular cross section and neglected the increase in stiffness of the material in cell and considered it to be an open cell foam. They concluded that the squared dependence on the relative density was mainly due to the bending.

Gent and Thomas (1959) considered two cases of thin threads of 3D network (Small strains and finite compressions) obtained by joining their ends to study the behavior of elastic foam materials. They analyzed the behavior based by developing a relation between the young's modulus and the foam density. Densities ranging from 0.09-0.57 were considered and tensile and compressive tests were conducted assuming the axial-only effects. Their theory showed satisfactory agreement with the experimental data.

Like Gent and Thomas (1959) Leaderman (1971) proposed a similar model by replacing the bars and nodes and his results fairly agreed with the experimental data.

Christensen (1986) studied three-dimensional isotropic material. He studied both open and closed cell foam. The cell edges are assumed to be axial bar for open cell foam and plane stress membrane for closed cell foam. The results showed that the Poisson's ratio was constant, and the shear modulus, elastic modulus and bulk modulus depends linearly on the relative density of the foam. By using his theory, he calculated the higher end value of the elastic modulus of Gibson and Ashby (1982).

2.4.2 NUMERICAL MODELS

Li et al (2005) found the formula for effective Young's modulus, Poisson's ratio and shear moduli of open cell foams. They used homogenization and by the matrix method for spatial frames by analyzing four cross sections of tetrakaidekahedral cell. The load cases that was studied is shown in figure 2.4. Three extreme load cases were observed namely when loads are applied perpendicular to two parallel square faces, loads are applied perpendicular to two parallel hexagonal faces and when loads are applied along the line connecting the nodes on the side opposite to the parallel square faces which gives the longest cell length. They found their results to be in contradiction with Zhu et al (1997).

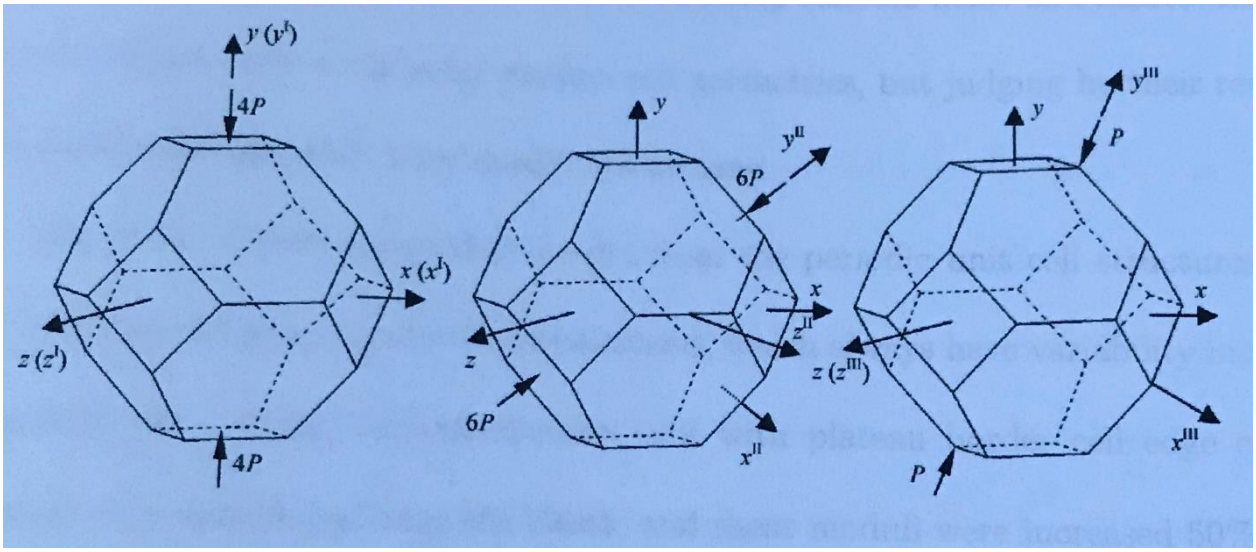

Figure 2.4: Load cases used by Li et al (2005). Case 1 (Left) Case 2 (Center) Case 3 (Right).

Maruyama et al (2006) were the first to estimate the elastic properties of actual foam structures. They determined the exact structure of AFRL foam which is a pitch-based carbon foam using a tool Robo-Met.3D. This tool helps in automated serial-sectioning techniques. Using ALGOR software the solid model was converted to a STEP AP 203 format to do the FE analysis to find the elastic stiffness and thermal conductivity.

Gan et al (2005) developed a three-dimensional Voronoi model as shown in figure 2.5 to examine the mechanical performance of linearly elastic open cell foams. Using Voronoi tessellations FEM model has been created and the Young's modulus, shear modulus and bulk modulus are estimated through the analysis. They found that Kelvin foams can be used to well represent the Voronoi foams however young's modulus and bulk modulus have some sensitive nature towards geometric imperfections. Whereas the plateau stress is insensitive. When cell edges are subjected to elastic buckling it causes compressive failure of the foam structure.

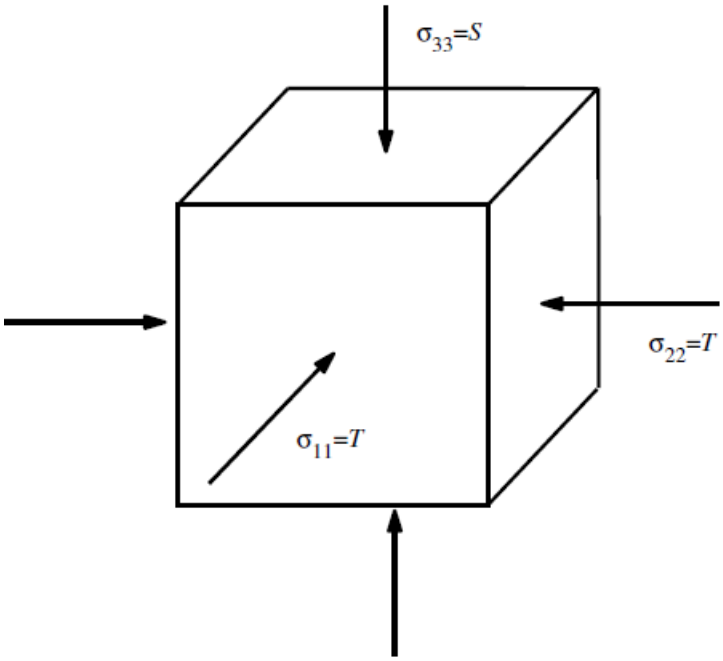

Figure 2.5: Three-dimensional loading imposed on the open cell Voronoi foams. (Gan et al, 2005).

Sihn and Roy (2004) performed a parametric study on tetrahedral carbon foam using 3D FE analysis. They figured that the bending associated with shear deformation dominated the effective elastic property of the foam and the ligament moduli influence the Young's modulus. The model was analyzed using ANSYS and their results has better correlation with other numerical experiments on carbon foams.

Gong et al (2005) studied polyester urethane foams using Bloch wave theory to find the critical stress limits for uniaxial and triaxial loadings. Their results were like Sihn and Roy (2004) and they showed that foam anisotropy is highly dependent on the buckling modes. They obtained the output by idealizing Kelvin foams to be periodic and space filling.

Van der Burg et al (1997) analyzed random geometries and found that the results agreed to the analytical models of Gibson and Ashby (1997) Warren and Kraynik (1997) when the relative densities are very low. But when the densities are increased the results showed error and it disagreed with the previous results. Struts which were smaller in dimension than the original length were removed, and the nodes were combined on both sides to make them as one node. This concluded that axial deformation of the struts should be considered. They found this deformation was caused by bending and the ratio of it depends on the magnitude of the density. They developed nodes having more than 4 edges joining at a point.

2.5 ELASTIC PROPERTIES OF 3D FOAMS

Roberts and Garboczi (2001) generated four random cell geometries using three models namely Voronoi tessellations, Level cut Gaussian random fields and nearest neighbor node bond rules. By varying the exponent n where n is greater than 1.3 and less than 3.0 and constant of proportionality based on the formation of structure the elastic modulus that relates to the relative density is determined. They figured out the overall Poisson's ratio was independent of the density

and at low densities three out of four models the Poisson's ratio converged to 0.25 and is incompressible due to the stiff nature under uniform compression than shear deformation. The results obtained were coinciding with the results of Warren and Kraynik's result on tetrahedral joint. However, the model has few issues with the random cell geometry between Gaussian and nearest neighbor node bond rules. In this study, it has been shown that it is necessary to consider large-scale (multi-cellular) models of random cellular solids to obtain realistic elastic properties.

Roberts and Garboczi (2002) contradicted the proposal of Christensen (1986). They generated the theoretical results for the Young's modulus for random models to study the properties of open cell solids. They selected four different isotropic random models based on Voronoi tessellations, level cut Gaussian random fields and nearest neighbor node bond rules. They compared the output with existing and experimental results. The results showed that the deformation was caused by axial tension rather than by bending. At low densities the poisson's ratio converged from 0.33 to 0.25. At low densities Open cell Voronoi tessellations were incompressible since structure is stiffer under compression than shear deformation. To obtain realistic elastic properties it is important to consider large scale models of random cellular solids. The elastic modulus was found to be three times lower than the actual value.

Warren and Kraynik (1988) analyzed a tetrahedral unit cell. Each unit cell has four identical half struts which forms the necessary microstructural by joining at equal angles. The cell edges were assumed to be a triangular cross section like Gibson and Ashby (1982). They also carried out the same experiment on the cubic microstructure that has six members joining at the nodes and calculated the relation between the elastic constant and relative density. The young's modulus was found to be proportional to the volume fraction of squared material for the uniform strut cross section.

Warren and Kraynik (1997) extended their previous analysis by studying foams having Kelvin soap froth geometry i.e.) there are 14 polyhedral cells each contains 6 squares and 8 hexagons. Periodic structure of this is obtained only when 4 cell edges meets together at the nodes and when these are stacked it should completely fill the volume. The results showed good agreement with their previous work. Among the various cross sections examined the Plateau border gave the stiffness result. Using this the elastic modulus is derived as

$$\frac{E^*}{E_S} = 0.979\left(\frac{\rho^*}{\rho_s}\right)^2 \tag{2.4}$$

Zhu et al (1997) did comparable analysis to Warren and Kraynik (1997) using body centered cubic lattice. They studied the elastic properties of Kelvin foams having tetrakaidekahedral cells. The practices used were different from Warren and Kraynik (1988) and found that the Young's modulus obtained by them were 51% greater than this structure at low density. In general, these foams are anisotropic, but they considered their lattice to be isotropic. At this low density their results matched exactly with Dement'ev and Tarakanova's (1970b) prediction for the young's modulus. However, this was later opposed by Li et al (2005).

Zhu et al (1997) developed the equation for the elastic modulus assuming plateau borders in the strong direction of cell edges as

$$\frac{E^*}{E_s} = \frac{1.009\left(\frac{\rho^*}{\rho_s}\right)^2}{1 + 1.514\left(\frac{\rho^*}{\rho_s}\right)} \tag{2.5}$$

2.6 OTHER SMART MATERIAL COMPOSITES

Dunn and Taya (1993) developed a matrix formulation to calculate the effective electrostatic moduli and electromechanical properties of porous piezoelectric ceramics. Properties such as elastic, dielectric and the electro-elastic moduli were analyzed under the effect of porosity

volume fraction and the results showed that with the increase of the porosity volume fraction, there was a decrease in the moduli.

Huang et.al (2009) were the first to study the behavior of magneto electro elastic materials under the presence of any defects. By using Eshelby's equivalent principle they studied the effective properties of MEE composites under the influence of ellipsoidal voids. The results proved that the effective properties are weakened due to the void volume fraction and void orientation. However, they had some limitations with the Eshelby's equation, and the procedure followed cannot be used when the voids are densely distributed.

Iyer and Venkatesh (2014) Predicted the elastic, dielectric and piezoelectric properties of piezoelectric composites (0-3) and (1-3) having anisotropic constituents by developing an analytical background by homogenization method. In figure 2.6, the different shapes of unit cells such as hexagonal and rectangle used in this study is shown. The results were validated with the FEM for a range of piezoelectric composites having various degrees of anisotropy in elastic and piezoelectric activity and found that it has good agreement with Dunn and Taya (1993). With increase in porosity volume fraction there was a decrease in the dielectric and piezoelectric constant.

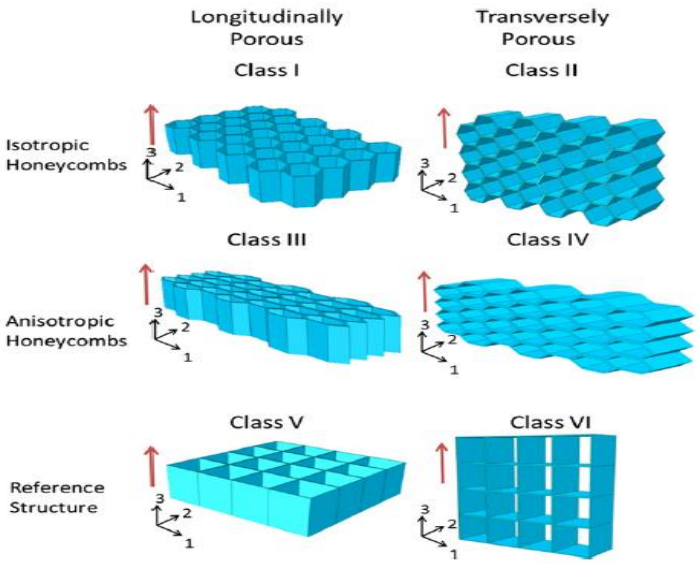

Figure 2.6: Sketch of 4 classes of piezoelectric honeycomb structure and two classes of reference foam. (Iyer et al, 2014).

2.7 SIGNIFICANCE OF THIS RESEARCH

The present study emphases on modelling a three-dimensional cellular foam composed of MEE composites using finite element method in order to discover its effective properties such as elastic coefficients and the effective coupled coefficients like piezoelectric and piezomagnetic for different shapes of unit cell. The obtained results will be plotted as a graph against relative density and the obtained results will be presented for any new or future studies.

CHAPTER 3

METHODOLOGY

All the governing equations, the boundary conditions and the procedure used to do the analyzing the various parameters of the foams are explained in this chapter.

3.1 CONFIGURATION OF CELLULAR STRUCTURE

The very first step of finite element analysis is defining the element position and their connectivity. All the elements are numbered, and the nodes are numbered in a particular pattern in order to form the element connectivity. Investigation of the various parameters such as elastic, piezoelectric and piezomagnetic properties of the cellular foams is the main goal of this research and hence all the structures that are being analyzed are three dimensional. The elements in the global structure lay in a single three-dimensional plane which is represented as X-Y-Z plane in this thesis.

The structure used in this thesis resembles the structure of a three-dimensional jack packed cell. The cell thickness to length ratio is increased at each analysis and it varies between the range of 0.2-1.0. The Poisson's ratio assumed in this research is ranges from 0.1-0.4. For each Poisson's ratio and thickness of the foam, the analysis is carried out to get the effective properties.

3.2 GOVERNING EQUATIONS

The main governing equation for this analysis is the equations of equilibrium in the rectangular Cartesian coordinates and in the absence of electric and magnetic field the components of electric and magnetic displacements D_i and B_i respectively are given by the quasi-static Maxwell equations

The indicial form of this differential equations of equilibrium equation can be expresses as:

$$\sigma_{ij,j} + f_i = 0 \tag{3.1}$$

Where σ_{ij} are the stress components and f_i are the body forces.

The components of electric and magnetic displacements D_i and B_i respectively are given by the quasi-static Maxwell equations as follows

$$D_{i,i} = 0 \tag{3.2}$$

$$B_{i,i} = 0 \tag{3.3}$$

In a linear MEE solid and for the foam structure considered in this research the constitutive equations are given as:

$$\sigma_{ij} = C_{ijkl}S_{kl} - e_{kij}E_k - q_{kij}H_k \tag{3.4}$$

$$D_m = e_{mkl}S_{kl} + \epsilon_{mk}E_k + d_{mk}H_k \tag{3.5}$$

$$B_m = q_{mkl}S_{kl} + d_{mk}E_k + \mu_{mk}H_k \tag{3.6}$$

Where

C_{ijkl} is the elastic coefficient, e_{kij} is the piezoelectric coefficient, q_{kij} is the piezo magnetic coefficient, E_k is the electric field, H_k is the magnetic field, , σ_{ij} , D_m and B_m are the components of stress, electric displacement and magnetic induction respectively, S_{kl} , E_k and H_k are respectively the components of strain, electric and magnetic field, ϵ_{mk} is the dielectric coefficient and μ_{mk} is the magnetic permeability, d_{mk} is the magnetoelectric coefficient.

Assuming small displacement theory the strain-displacement relations can be written as

$$\epsilon_{XX} = \frac{\partial u}{\partial x} \tag{3.7}$$

$$\epsilon_{YY} = \frac{\partial v}{\partial y} \tag{3.8}$$

$$\gamma_{XY} = \frac{\partial v}{\partial x} + \frac{\partial u}{\partial y} \tag{3.9}$$

where ϵ_{XX} and ϵ_{YY} are the components of the linear strain tensor in the normal direction and γ_{XY} are the components of engineering shear strain.

The electric field components are given by

$$E_i = \frac{\partial \phi}{\partial x_i} \tag{3.10}$$

where ϕ is the electrostatic potential.

The magnetic induction is by its relation to magnetic potential as

$$B_i = \frac{\partial \psi}{\partial x_i} \tag{3.11}$$

where ψ is the magnetic potential.

In these equations the indices i and j which represents the rectangular Cartesian Coordinates ranges from 1 to 3. In a linear theory, a reduced notation in standard fashion that uses single subscript instead of double subscript for the stress components is commonly used. The standard mapping that is used to replace these indices is as follows

ij	=	11	22	33	23,32	13,31	12,21
⇩		⇩	⇩	⇩	⇩	⇩	⇩
α	=	1	2	3	4	5	6

It is also noted that $C_{ijkl} = C_{ijlk} = C_{jikl}$, $e_{ijk} = e_{ikj}$, $q_{ijk} = q_{ikj}$, $\sigma_{ij} = \sigma_{ji}$. The elastic stiffness in the final form are given as C_{11}, C_{22} , C_{33} , C_{44}, C_{55}, C_{66}, C_{12}, C_{13}, C_{23}.

3.3 HOMOGENIZATION

The most commonly used technique for composite material is the homogenization. The entire solid will be divided into small elements. This procedure is carried out in such a way that each small element is a repeating unit cell (RUC) or the representative volume element (RVE) of the entire solid and is explained in figure 3.1.

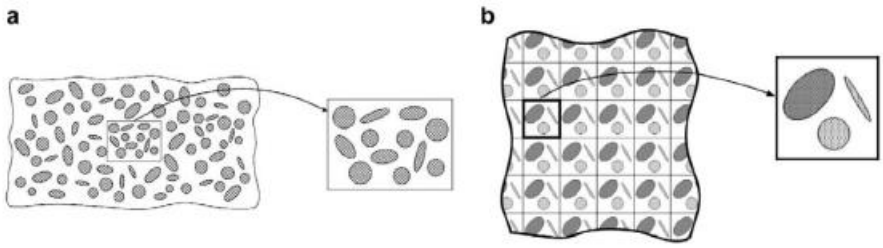

Figure 3.1: Microstructure of material representation (a) RVE of statistically homogenous material. (b) Periodic microstructure identified by RUC. (Pindera et al, 2009).

3.4 FINITE ELEMENT METHOD

Finite element approximations were used to solve the equations that are being used in this study. FE approximations is the commonly used technique and it is one of the powerful tools to solve structures that has complicated geometries.

3.4.1 DISCRETIZATION

Discretization of the solid is the primary step in any FEM analysis. The entire structure is discretized into small elements. These elements are connected and are numbered at each joint

which is known commonly as node numbers. Each joint or node has their own degrees of freedom based on the parameters that are considered for the study. Each element is identified by their node connectivity which is done by numbering either clockwise or in anti-clockwise direction. In this study anti clockwise connectivity is considered. For this research an eight nodded is considered to discretize the unit cell of the three-dimensional cellular foams. Each node will have five degrees of freedom as follows:

Displacement in the X1 direction represented by u, Displacement in the X2 direction represented by v, Displacement in the X3 direction represented by w, the electric potential and the magnetic potential. Different boundary conditions are used to find these degrees of freedom and a more accurate value can be obtained by increasing the number of nodes thus making each unit element much smaller in size. However, by doing this the problem becomes more difficult and it takes a longer processing time. The shape that resembles our foam structure used in this study has been shown in figure 3.2. This shows exactly a unit cell representation of the foam structure under study. Each unit cell has 8 nodes and each node has 5 degrees of freedom. Figure 3.3 shows the three-dimensional jack packed shaped cellular foam that was used in the research. Figure 3.3 (A) shows the foams structure at thickness to length ratio of 0.2 and 3.3(B) represents for t/l ratio of 0.4 and 3.3(C) represents for t/l ratio of 0.6. When we consider a t/l ratio of 1.0 the structure of the foam changes into a perfect cube made of repeating unit cells of jack packed shape.

Figure 3.2: Shape resemble to that of the three - dimensional jack foam.

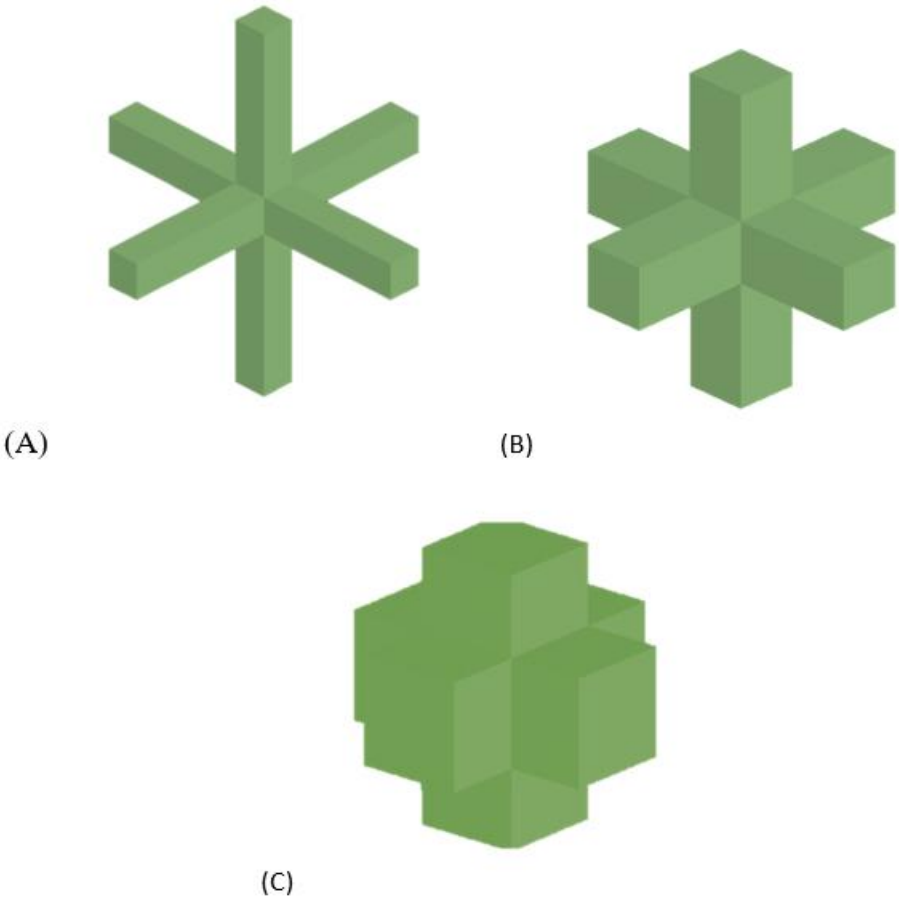

Figure 3.3: Different thickness of jack packed foam structure used in this research (A) t/l = 0.2 (B) t/l = 0.4 (C) t/l = 0.6.

3.4.2 WEAK FORM

Forming the weak form is the next step in FEM analysis. An arbitrary function is multiplied to the original governing equation, integrated over a domain and equaled to zero. This makes the continuity and the differential equations less complicated to work with.

To start with the weak form the equilibrium equations are expanded and then integrating by parts and substituting the corresponding terms the element matrix is obtained.

The equilibrium equations are as follows

$$\frac{\partial}{\partial x}\,\sigma_{xx} + \frac{\partial}{\partial y}\,\sigma_{xy} + \frac{\partial}{\partial z}\,\sigma_{xz} + f_x = 0 \tag{3.12}$$

$$\frac{\partial}{\partial x}\,\sigma_{xy} + \frac{\partial}{\partial y}\,\sigma_{yy} + \frac{\partial}{\partial z}\,\sigma_{yz} + f_y = 0 \tag{3.13}$$

$$\frac{\partial}{\partial x}\,\sigma_{xz} + \frac{\partial}{\partial y}\,\sigma_{yz} + \frac{\partial}{\partial z}\,\sigma_{zz} + f_z = 0 \tag{3.14}$$

For the piezoelectric and piezomagnetic parameters the equation of equilibrium are as follows

$$\frac{\partial}{\partial x}\,D_1 + \frac{\partial}{\partial y}\,D_2 + \frac{\partial}{\partial z}\,D_3 = 0 \tag{3.15}$$

$$\frac{\partial}{\partial x}\,\mathrm{B}_1 + \frac{\partial}{\partial y}\,B_2 + \frac{\partial}{\partial z}\,B_3 = 0 \tag{3.16}$$

Integrating by parts and expanding all these sets of equilibrium equations we get the following sets of equations.

$$
\begin{aligned}
0 = \int_V \Big\{ & \frac{-\partial W_1}{\partial x}\left[C_{11}\left(\frac{\partial u}{\partial x}\right) + C_{12}\left(\frac{\partial v}{\partial y}\right) + C_{13}\left(\frac{\partial w}{\partial z}\right) + C_{16}\left(\frac{\partial u}{\partial y} + \frac{\partial v}{\partial x}\right)\right. \\
& \left. - e_{31}\left(\frac{\partial \phi}{\partial z}\right) - q_{31}\left(\frac{\partial \psi}{\partial z}\right)\right] \\
& - \frac{\partial W_1}{\partial y}\left[C_{16}\left(\frac{\partial u}{\partial x}\right) + C_{26}\left(\frac{\partial v}{\partial y}\right) + C_{36}\left(\frac{\partial w}{\partial z}\right) + C_{66}\left(\frac{\partial u}{\partial y} + \frac{\partial v}{\partial x}\right)\right] \\
& - \frac{\partial W_1}{\partial z}\left[C_{45}\left(\frac{\partial v}{\partial z} + \frac{\partial w}{\partial y}\right) + C_{55}\left(\frac{\partial u}{\partial z} + \frac{\partial w}{\partial x}\right) - e_{15}\left(\frac{\partial \phi}{\partial x}\right)\right. \\
& \left. - q_{15}\left(\frac{\partial \psi}{\partial x}\right)\right] + f_x W_1 \Big\} dxdydz + \oint_{\mu^e} W_1 t_x ds
\end{aligned} \tag{3.17}
$$

$$
\begin{aligned}
0 = \int_V \; & C_{11}\left(\frac{\partial W_1}{\partial x}\,\frac{\partial u}{\partial x}\right) + C_{12}\left(\frac{\partial W_1}{\partial x}\,\frac{\partial v}{\partial y}\right) + C_{13}\left(\frac{\partial W_1}{\partial x}\,\frac{\partial w}{\partial z}\right) \\
& + C_{16}\left(\frac{\partial W_1}{\partial x}\,\frac{\partial u}{\partial y} + \frac{\partial W_1}{\partial x}\,\frac{\partial v}{\partial x}\right) + e_{31}\left(\frac{\partial W_1}{\partial x}\,\frac{\partial \phi}{\partial z}\right) \\
& + q_{31}\left(\frac{\partial W_1}{\partial x}\,\frac{\partial \psi}{\partial z}\right) + C_{16}\left(\frac{\partial W_1}{\partial y}\,\frac{\partial u}{\partial x}\right) + C_{26}\left(\frac{\partial W_1}{\partial y}\,\frac{\partial v}{\partial y}\right) \\
& + C_{36}\left(\frac{\partial W_1}{\partial y}\,\frac{\partial w}{\partial z}\right) + C_{66}\left(\frac{\partial W_1}{\partial y}\,\frac{\partial u}{\partial y} + \frac{\partial W_1}{\partial y}\,\frac{\partial v}{\partial x}\right) \\
& + C_{45}\left(\frac{\partial W_1}{\partial z}\,\frac{\partial v}{\partial z} + \frac{\partial W_1}{\partial z}\,\frac{\partial w}{\partial y}\right) + C_{55}\left(\frac{\partial W_1}{\partial z}\,\frac{\partial u}{\partial z} + \frac{\partial W_1}{\partial z}\,\frac{\partial w}{\partial x}\right) \\
& - e_{15}\left(\frac{\partial W_1}{\partial z}\,\frac{\partial \phi}{\partial x}\right) - q_{15}\left(\frac{\partial W_1}{\partial z}\,\frac{\partial \psi}{\partial x}\right) dxdydz
\end{aligned} \tag{3.18}
$$

$$
\begin{aligned}
0 = \int_V \Big\{ & \frac{-\partial W_2}{\partial x}\left[C_{16}\left(\frac{\partial u}{\partial x}\right) + C_{26}\left(\frac{\partial v}{\partial y}\right) + C_{36}\left(\frac{\partial w}{\partial z}\right) + C_{66}\left(\frac{\partial u}{\partial y} + \frac{\partial v}{\partial x}\right)\right] \\
& - \frac{\partial W_2}{\partial y}\left[C_{12}\left(\frac{\partial u}{\partial x}\right) + C_{22}\left(\frac{\partial v}{\partial y}\right) + C_{23}\left(\frac{\partial w}{\partial z}\right) + C_{26}\left(\frac{\partial u}{\partial y} + \frac{\partial v}{\partial x}\right)\right. \\
& \left. - e_{32}\left(\frac{\partial \phi}{\partial z}\right) - q_{32}\left(\frac{\partial \psi}{\partial z}\right)\right] \\
& - \frac{\partial W_2}{\partial z}\left[C_{44}\left(\frac{\partial v}{\partial z} + \frac{\partial w}{\partial y}\right) + C_{45}\left(\frac{\partial u}{\partial z} + \frac{\partial w}{\partial x}\right) - e_{24}\left(\frac{\partial \phi}{\partial y}\right)\right. \\
& \left. - q_{24}\left(\frac{\partial \psi}{\partial y}\right)\right] + f_y W_2 \Big\} dxdydz + \oint_{\mu^e} W_2 t_y ds
\end{aligned} \tag{3.19}
$$

$$
\begin{aligned}
0 = \int_V \; & C_{16}\left(\frac{\partial W_2}{\partial x}\,\frac{\partial u}{\partial x}\right) + C_{26}\left(\frac{\partial W_2}{\partial x}\,\frac{\partial v}{\partial y}\right) + C_{36}\left(\frac{\partial W_2}{\partial x}\,\frac{\partial w}{\partial z}\right) \\
& + C_{66}\left(\frac{\partial W_2}{\partial x}\,\frac{\partial u}{\partial y} + \frac{\partial W_2}{\partial x}\,\frac{\partial v}{\partial x}\right) + C_{12}\left(\frac{\partial W_2}{\partial y}\,\frac{\partial u}{\partial x}\right) \\
& + C_{22}\left(\frac{\partial W_2}{\partial y}\,\frac{\partial v}{\partial y}\right) + C_{23}\left(\frac{\partial W_2}{\partial y}\,\frac{\partial w}{\partial z}\right) \\
& + C_{26}\left(\frac{\partial W_2}{\partial y}\,\frac{\partial u}{\partial y} + \frac{\partial W_2}{\partial y}\,\frac{\partial v}{\partial x}\right) + e_{32}\left(\frac{\partial W_2}{\partial y}\,\frac{\partial \phi}{\partial z}\right) \\
& + q_{32}\left(\frac{\partial W_2}{\partial y}\,\frac{\partial \psi}{\partial z}\right) + C_{44}\left(\frac{\partial W_2}{\partial z}\,\frac{\partial v}{\partial z} + \frac{\partial W_2}{\partial z}\,\frac{\partial w}{\partial y}\right) \\
& + C_{45}\left(\frac{\partial W_2}{\partial z}\,\frac{\partial u}{\partial z} + \frac{\partial W_2}{\partial z}\,\frac{\partial w}{\partial x}\right) + e_{24}\left(\frac{\partial W_2}{\partial z}\,\frac{\partial \phi}{\partial y}\right) \\
& + q_{24}\left(\frac{\partial W_2}{\partial z}\,\frac{\partial \psi}{\partial y}\right) dxdydz
\end{aligned}
\tag{3.20}
$$

$$
\begin{aligned}
0 = \int_V \; & \left\{ \frac{-\partial W_3}{\partial x}\left[C_{45}\left(\frac{\partial v}{\partial z} + \frac{\partial w}{\partial y}\right) + C_{55}\left(\frac{\partial u}{\partial z} + \frac{\partial w}{\partial x}\right) - e_{15}\left(\frac{\partial \phi}{\partial x}\right) \right.\right. \\
& \left. - q_{15}\left(\frac{\partial \psi}{\partial x}\right)\right] \\
& - \frac{\partial W_3}{\partial y}\left[C_{44}\left(\frac{\partial v}{\partial z} + \frac{\partial w}{\partial y}\right) + C_{45}\left(\frac{\partial u}{\partial z} + \frac{\partial w}{\partial x}\right) - e_{24}\left(\frac{\partial \phi}{\partial y}\right) \right. \\
& \left. - q_{24}\left(\frac{\partial \psi}{\partial y}\right)\right] \\
& - \frac{\partial W_3}{\partial z}\left[C_{13}\left(\frac{\partial u}{\partial x}\right) + C_{36}\left(\frac{\partial u}{\partial y} + \frac{\partial v}{\partial x}\right) - e_{33}\left(\frac{\partial \phi}{\partial z}\right) \right. \\
& \left.\left. - q_{33}\left(\frac{\partial \psi}{\partial z}\right)\right] + f_z W_3 \right\} dxdydz + \oint_{\mu^e} W_3 t_z ds
\end{aligned}
\tag{3.21}
$$

$$
\begin{aligned}
0 = \int_V \; & C_{45}\left(\frac{\partial W_3}{\partial x}\,\frac{\partial v}{\partial z}+\frac{\partial W_3}{\partial x}\,\frac{\partial w}{\partial y}\right)+C_{55}\left(\frac{\partial W_3}{\partial x}\,\frac{\partial u}{\partial z}+\frac{\partial W_3}{\partial x}\,\frac{\partial w}{\partial x}\right)\\
&+e_{15}\left(\frac{\partial W_3}{\partial x}\,\frac{\partial \phi}{\partial x}\right)\\
&+q_{15}\left(\frac{\partial W_3}{\partial x}\,\frac{\partial \psi}{\partial x}\right)+C_{44}\left(\frac{\partial W_3}{\partial y}\,\frac{\partial v}{\partial z}+\frac{\partial W_3}{\partial y}\,\frac{\partial w}{\partial y}\right)\\
&+C_{45}\left(\frac{\partial W_3}{\partial y}\,\frac{\partial u}{\partial z}+\frac{\partial W_3}{\partial y}\,\frac{\partial w}{\partial x}\right)+e_{24}\left(\frac{\partial W_3}{\partial y}\,\frac{\partial \phi}{\partial y}\right)\\
&+q_{24}\left(\frac{\partial W_3}{\partial y}\,\frac{\partial \psi}{\partial y}\right)+C_{13}\left(\frac{\partial W_3}{\partial z}\,\frac{\partial u}{\partial x}\right)+C_{13}\left(\frac{\partial W_3}{\partial z}\,\frac{\partial v}{\partial y}\right)\\
&+C_{36}\left(\frac{\partial W_3}{\partial z}\,\frac{\partial u}{\partial y}+\frac{\partial W_3}{\partial z}\,\frac{\partial v}{\partial x}\right)+e_{33}\left(\frac{\partial W_3}{\partial z}\,\frac{\partial \phi}{\partial z}\right)\\
&+q_{33}\left(\frac{\partial W_3}{\partial z}\,\frac{\partial \psi}{\partial z}\right)dxdydz
\end{aligned}
\tag{3.22}
$$

$$
\begin{aligned}
0 = \int_V \; & \left\{\frac{-\partial W_4}{\partial x}\left[e_{11}\left(\frac{\partial u}{\partial x}\right)+e_{21}\left(\frac{\partial v}{\partial y}\right)+e_{31}\left(\frac{\partial w}{\partial z}\right)+e_{12}\left(\frac{\partial v}{\partial z}+\frac{\partial w}{\partial y}\right)\right.\right.\\
&+e_{22}\left(\frac{\partial u}{\partial z}+\frac{\partial w}{\partial x}\right)+e_{32}\left(\frac{\partial u}{\partial y}+\frac{\partial v}{\partial x}\right)+\epsilon_{11}\left(\frac{\partial \phi}{\partial x}\right)+\epsilon_{12}\left(\frac{\partial \phi}{\partial y}\right)\\
&\left.+\epsilon_{13}\left(\frac{\partial \phi}{\partial z}\right)+d_{11}\left(\frac{\partial \psi}{\partial x}\right)+d_{12}\left(\frac{\partial \psi}{\partial y}\right)+d_{13}\left(\frac{\partial \psi}{\partial z}\right)\right]\\
&-\frac{\partial W_4}{\partial y}\left[e_{13}\left(\frac{\partial u}{\partial x}\right)+e_{23}\left(\frac{\partial v}{\partial y}\right)+e_{33}\left(\frac{\partial w}{\partial z}\right)+e_{14}\left(\frac{\partial v}{\partial z}+\frac{\partial w}{\partial y}\right)\right.\\
&+e_{24}\left(\frac{\partial u}{\partial z}+\frac{\partial w}{\partial x}\right)+e_{34}\left(\frac{\partial u}{\partial y}+\frac{\partial v}{\partial x}\right)+\epsilon_{21}\left(\frac{\partial \phi}{\partial x}\right)+\epsilon_{22}\left(\frac{\partial \phi}{\partial y}\right)\\
&\left.+\epsilon_{23}\left(\frac{\partial \phi}{\partial z}\right)+d_{21}\left(\frac{\partial \psi}{\partial x}\right)+d_{22}\left(\frac{\partial \psi}{\partial y}\right)+d_{33}\left(\frac{\partial \psi}{\partial z}\right)\right]\\
&-\frac{\partial W_4}{\partial z}\left[e_{15}\left(\frac{\partial u}{\partial x}\right)+e_{25}\left(\frac{\partial v}{\partial y}\right)+e_{35}\left(\frac{\partial w}{\partial z}\right)+e_{16}\left(\frac{\partial v}{\partial z}+\frac{\partial w}{\partial y}\right)\right.\\
&+e_{26}\left(\frac{\partial u}{\partial z}+\frac{\partial w}{\partial x}\right)+e_{36}\left(\frac{\partial u}{\partial y}+\frac{\partial v}{\partial x}\right)+\epsilon_{31}\left(\frac{\partial \phi}{\partial x}\right)+\epsilon_{32}\left(\frac{\partial \phi}{\partial y}\right)\\
&\left.\left.+\epsilon_{33}\left(\frac{\partial \phi}{\partial z}\right)+d_{31}\left(\frac{\partial \psi}{\partial x}\right)+d_{32}\left(\frac{\partial \psi}{\partial y}\right)+d_{33}\left(\frac{\partial \psi}{\partial z}\right)\right]\right\}dxdydz\\
&+\oint_{\mu^e} W_4\left(D_1 n_x+D_2 n_y+D_3 n_z\right)ds
\end{aligned}
\tag{3.23}
$$

$$
\begin{aligned}
0 = \int_V \; & e_{11}\left(\frac{\partial W_4}{\partial x}\,\frac{\partial u}{\partial x}\right) + e_{21}\left(\frac{\partial W_4}{\partial x}\,\frac{\partial v}{\partial y}\right) + e_{31}\left(\frac{\partial W_4}{\partial x}\,\frac{\partial w}{\partial z}\right) \\
& + e_{12}\left(\frac{\partial W_4}{\partial x}\,\frac{\partial v}{\partial z} + \frac{\partial W_4}{\partial x}\,\frac{\partial w}{\partial y}\right) + e_{22}\left(\frac{\partial W_4}{\partial x}\,\frac{\partial u}{\partial z} + \frac{\partial W_4}{\partial x}\,\frac{\partial w}{\partial x}\right) \\
& + e_{32}\left(\frac{\partial W_4}{\partial x}\,\frac{\partial u}{\partial y} + \frac{\partial W_4}{\partial x}\,\frac{\partial v}{\partial x}\right) + \epsilon_{11}\left(\frac{\partial W_4}{\partial x}\,\frac{\partial \phi}{\partial x}\right) \\
& + \epsilon_{12}\left(\frac{\partial W_4}{\partial x}\,\frac{\partial \phi}{\partial y}\right) + \epsilon_{13}\left(\frac{\partial W_4}{\partial x}\,\frac{\partial \phi}{\partial z}\right) + d_{11}\left(\frac{\partial W_4}{\partial x}\,\frac{\partial \psi}{\partial x}\right) \\
& + d_{12}\left(\frac{\partial W_4}{\partial x}\,\frac{\partial \psi}{\partial y}\right) + d_{13}\left(\frac{\partial W_4}{\partial x}\,\frac{\partial \psi}{\partial z}\right) \\
& + e_{13}\left(\frac{\partial W_4}{\partial y}\,\frac{\partial u}{\partial x}\right) + e_{23}\left(\frac{\partial W_4}{\partial y}\,\frac{\partial v}{\partial y}\right) \\
& + e_{33}\left(\frac{\partial W_4}{\partial y}\,\frac{\partial w}{\partial z}\right) + e_{14}\left(\frac{\partial W_4}{\partial y}\,\frac{\partial v}{\partial z} + \frac{\partial W_4}{\partial y}\,\frac{\partial w}{\partial y}\right) \\
& + e_{24}\left(\frac{\partial W_4}{\partial y}\,\frac{\partial u}{\partial z} + \frac{\partial W_4}{\partial y}\,\frac{\partial u}{\partial z}\right) + e_{34}\left(\frac{\partial W_4}{\partial y}\,\frac{\partial u}{\partial y} + \frac{\partial W_4}{\partial y}\,\frac{\partial v}{\partial x}\right) \\
& + \epsilon_{21}\left(\frac{\partial W_4}{\partial y}\,\frac{\partial \phi}{\partial x}\right) + \epsilon_{22}\left(\frac{\partial W_4}{\partial y}\,\frac{\partial \phi}{\partial y}\right) + \epsilon_{23}\left(\frac{\partial W_4}{\partial y}\,\frac{\partial \phi}{\partial z}\right) \\
& + d_{21}\left(\frac{\partial W_4}{\partial y}\,\frac{\partial \psi}{\partial x}\right) + d_{22}\left(\frac{\partial W_4}{\partial y}\,\frac{\partial \psi}{\partial y}\right) + d_{33}\left(\frac{\partial W_4}{\partial y}\,\frac{\partial \psi}{\partial z}\right) \\
& + e_{15}\left(\frac{\partial W_4}{\partial z}\,\frac{\partial u}{\partial x}\right) + e_{25}\left(\frac{\partial W_4}{\partial z}\,\frac{\partial v}{\partial y}\right) + e_{35}\left(\frac{\partial W_4}{\partial z}\,\frac{\partial w}{\partial z}\right) \\
& + e_{16}\left(\frac{\partial W_4}{\partial z}\,\frac{\partial u}{\partial z} + \frac{\partial W_4}{\partial z}\,\frac{\partial w}{\partial y}\right) + e_{26}\left(\frac{\partial W_4}{\partial z}\,\frac{\partial u}{\partial z} + \frac{\partial W_4}{\partial z}\,\frac{\partial w}{\partial x}\right) \\
& + e_{36}\left(\frac{\partial W_4}{\partial z}\,\frac{\partial u}{\partial y} + \frac{\partial W_4}{\partial z}\,\frac{\partial v}{\partial x}\right) + \epsilon_{31}\left(\frac{\partial W_4}{\partial z}\,\frac{\partial \phi}{\partial x}\right) \\
& + \epsilon_{32}\left(\frac{\partial W_4}{\partial z}\,\frac{\partial \phi}{\partial y}\right) + \epsilon_{33}\left(\frac{\partial W_4}{\partial z}\,\frac{\partial \phi}{\partial z}\right) + d_{31}\left(\frac{\partial W_4}{\partial z}\,\frac{\partial \psi}{\partial x}\right) \\
& + d_{32}\left(\frac{\partial W_4}{\partial z}\,\frac{\partial \psi}{\partial y}\right) + d_{33}\left(\frac{\partial W_4}{\partial z}\,\frac{\partial \psi}{\partial z}\right) dxdydz
\end{aligned}
\tag{3.24}
$$

$$
\begin{aligned}
0 = \int_V \Big\{ & \frac{-\partial W_5}{\partial x}\left[q_{11}\left(\frac{\partial u}{\partial x}\right) + q_{21}\left(\frac{\partial v}{\partial y}\right) + q_{31}\left(\frac{\partial w}{\partial z}\right) + q_{12}\left(\frac{\partial v}{\partial z} + \frac{\partial w}{\partial y}\right)\right. \\
& + q_{22}\left(\frac{\partial u}{\partial z} + \frac{\partial w}{\partial x}\right) + q_{32}\left(\frac{\partial u}{\partial y} + \frac{\partial v}{\partial x}\right) + d_{11}\left(\frac{\partial \phi}{\partial x}\right) + d_{12}\left(\frac{\partial \phi}{\partial y}\right) \\
& \left. + d_{13}\left(\frac{\partial \phi}{\partial z}\right) + \mu_{11}\left(\frac{\partial \psi}{\partial x}\right) + \mu_{12}\left(\frac{\partial \psi}{\partial y}\right) + \mu_{13}\left(\frac{\partial \psi}{\partial z}\right)\right] \\
& - \frac{\partial W_5}{\partial y}\left[q_{13}\left(\frac{\partial u}{\partial x}\right) + q_{23}\left(\frac{\partial v}{\partial y}\right) + q_{33}\left(\frac{\partial w}{\partial z}\right) + q_{14}\left(\frac{\partial v}{\partial z} + \frac{\partial w}{\partial y}\right)\right. \\
& + q_{24}\left(\frac{\partial u}{\partial z} + \frac{\partial w}{\partial x}\right) + q_{34}\left(\frac{\partial u}{\partial y} + \frac{\partial v}{\partial x}\right) + d_{21}\left(\frac{\partial \phi}{\partial x}\right) + d_{22}\left(\frac{\partial \phi}{\partial y}\right) \\
& \left. + d_{23}\left(\frac{\partial \phi}{\partial z}\right) + \mu_{21}\left(\frac{\partial \psi}{\partial x}\right) + \mu_{22}\left(\frac{\partial \psi}{\partial y}\right) + \mu_{33}\left(\frac{\partial \psi}{\partial z}\right)\right] \\
& - \frac{\partial W_5}{\partial z}\left[q_{15}\left(\frac{\partial u}{\partial x}\right) + q_{25}\left(\frac{\partial v}{\partial y}\right) + q_{35}\left(\frac{\partial w}{\partial z}\right) + q_{16}\left(\frac{\partial v}{\partial z} + \frac{\partial w}{\partial y}\right)\right. \\
& + q_{26}\left(\frac{\partial u}{\partial z} + \frac{\partial w}{\partial x}\right) + q_{36}\left(\frac{\partial u}{\partial y} + \frac{\partial v}{\partial x}\right) + d_{31}\left(\frac{\partial \phi}{\partial x}\right) + d_{32}\left(\frac{\partial \phi}{\partial y}\right) \\
& \left. + d_{33}\left(\frac{\partial \phi}{\partial z}\right) + \mu_{31}\left(\frac{\partial \psi}{\partial x}\right) + \mu_{32}\left(\frac{\partial \psi}{\partial y}\right) + \mu_{33}\left(\frac{\partial \psi}{\partial z}\right)\right]\Big\} dxdydz \\
& + \oint_{\mu^e} W_5\left(B_1 n_x + B_2 n_y + B_3 n_z\right) ds
\end{aligned}
\tag{3.25}
$$

$$
\begin{aligned}
0 = \int_V \; & q_{11}\left(\frac{\partial W_5}{\partial x}\,\frac{\partial u}{\partial x}\right) + q_{21}\left(\frac{\partial W_5}{\partial x}\,\frac{\partial v}{\partial y}\right) + q_{31}\left(\frac{\partial W_5}{\partial x}\,\frac{\partial w}{\partial z}\right) \\
& + q_{12}\left(\frac{\partial W_5}{\partial x}\,\frac{\partial v}{\partial z} + \frac{\partial W_5}{\partial x}\,\frac{\partial w}{\partial y}\right) + q_{22}\left(\frac{\partial W_5}{\partial x}\,\frac{\partial u}{\partial z} + \frac{\partial W_5}{\partial x}\,\frac{\partial w}{\partial x}\right) \\
& + q_{32}\left(\frac{\partial W_5}{\partial x}\,\frac{\partial u}{\partial y} + \frac{\partial W_5}{\partial x}\,\frac{\partial v}{\partial x}\right) + d_{11}\left(\frac{\partial W_5}{\partial x}\,\frac{\partial \phi}{\partial x}\right) \\
& + d_{12}\left(\frac{\partial W_5}{\partial x}\,\frac{\partial \phi}{\partial y}\right) + d_{13}\left(\frac{\partial W_5}{\partial x}\,\frac{\partial \phi}{\partial z}\right) + \mu_{11}\left(\frac{\partial W_5}{\partial x}\,\frac{\partial \psi}{\partial x}\right) \\
& + \mu_{12}\left(\frac{\partial W_5}{\partial x}\,\frac{\partial \psi}{\partial y}\right) + \mu_{13}\left(\frac{\partial W_5}{\partial x}\,\frac{\partial \psi}{\partial z}\right) \\
& + q_{13}\left(\frac{\partial W_5}{\partial y}\,\frac{\partial u}{\partial x}\right) + q_{23}\left(\frac{\partial W_5}{\partial y}\,\frac{\partial v}{\partial y}\right) \\
& + q_{33}\left(\frac{\partial W_5}{\partial y}\,\frac{\partial w}{\partial z}\right) + q_{14}\left(\frac{\partial W_5}{\partial y}\,\frac{\partial v}{\partial z} + \frac{\partial W_5}{\partial y}\,\frac{\partial w}{\partial y}\right) \\
& + q_{24}\left(\frac{\partial W_5}{\partial y}\,\frac{\partial u}{\partial z} + \frac{\partial W_5}{\partial y}\,\frac{\partial u}{\partial z}\right) + q_{34}\left(\frac{\partial W_5}{\partial y}\,\frac{\partial u}{\partial y} + \frac{\partial W_5}{\partial y}\,\frac{\partial v}{\partial x}\right) \\
& + d_{21}\left(\frac{\partial W_5}{\partial y}\,\frac{\partial \phi}{\partial x}\right) + d_{22}\left(\frac{\partial W_5}{\partial y}\,\frac{\partial \phi}{\partial y}\right) + d_{23}\left(\frac{\partial W_5}{\partial y}\,\frac{\partial \phi}{\partial z}\right) \\
& + \mu_{21}\left(\frac{\partial W_5}{\partial y}\,\frac{\partial \psi}{\partial x}\right) + \mu_{22}\left(\frac{\partial W_5}{\partial y}\,\frac{\partial \psi}{\partial y}\right) + \mu_{33}\left(\frac{\partial W_5}{\partial y}\,\frac{\partial \psi}{\partial z}\right) \\
& + q_{15}\left(\frac{\partial W_5}{\partial z}\,\frac{\partial u}{\partial x}\right) + q_{25}\left(\frac{\partial W_5}{\partial z}\,\frac{\partial v}{\partial y}\right) + q_{35}\left(\frac{\partial W_5}{\partial z}\,\frac{\partial w}{\partial z}\right) \\
& + q_{16}\left(\frac{\partial W_5}{\partial z}\,\frac{\partial u}{\partial z} + \frac{\partial W_5}{\partial z}\,\frac{\partial w}{\partial y}\right) + q_{26}\left(\frac{\partial W_5}{\partial z}\,\frac{\partial u}{\partial z} + \frac{\partial W_5}{\partial z}\,\frac{\partial w}{\partial x}\right) \\
& + q_{36}\left(\frac{\partial W_5}{\partial z}\,\frac{\partial u}{\partial y} + \frac{\partial W_5}{\partial z}\,\frac{\partial v}{\partial x}\right) + d_{31}\left(\frac{\partial W_5}{\partial z}\,\frac{\partial \phi}{\partial x}\right) \\
& + d_{32}\left(\frac{\partial W_5}{\partial z}\,\frac{\partial \phi}{\partial y}\right) + d_{33}\left(\frac{\partial W_5}{\partial z}\,\frac{\partial \phi}{\partial z}\right) + \mu_{31}\left(\frac{\partial W_5}{\partial z}\,\frac{\partial \psi}{\partial x}\right) \\
& + \mu_{32}\left(\frac{\partial W_5}{\partial z}\,\frac{\partial \psi}{\partial y}\right) + \mu_{33}\left(\frac{\partial W_5}{\partial z}\,\frac{\partial \psi}{\partial z}\right) dxdydz
\end{aligned}
\tag{3.26}
$$

The FE approximation can be seen below

$$u(x,y,z) = \sum_{j=1}^{n} u_j \, N_j^u(x,y,z) \tag{3.27}$$

$$\partial \mathrm{u} = \; N_j^u \tag{3.28}$$

$$v(x,y,z) = \sum_{j=1}^{n} v_j \, N_j^v(x,y,z) \tag{3.29}$$

$$\partial \mathrm{v} = \ N_j^v \tag{3.30}$$

$$w(x,y,z) = \sum_{j=1}^{n} w_j \, N_j^w(x,y,z) \tag{3.31}$$

$$\partial \mathrm{w} = \ N_j^w \tag{3.32}$$

$$\psi(x,y,z) = \sum_{j=1}^{n} \psi_j \, N_j^\psi(x,y,z) \tag{3.33}$$

$$\partial \psi = \ N_j^\psi \tag{3.34}$$

$$\phi(x,y,z) = \sum_{j=1}^{n} \phi_j \, N_j^\phi(x,y,z) \tag{3.35}$$

$$\partial \phi = \ N_j^\phi \tag{3.36}$$

ELEMENT MATRICES

$$\begin{Bmatrix} \{F^1\} \\ \{F^2\} \\ \{F^3\} \\ \{F^4\} \\ \{F^5\} \end{Bmatrix} = \begin{bmatrix} [K^{11}] & [K^{12}] & [K^{13}] & [K^{14}] & [K^{15}] \\ [K^{21}] & [K^{22}] & [K^{23}] & [K^{24}] & [K^{25}] \\ [K^{31}] & [K^{32}] & [K^{33}] & [K^{34}] & [K^{35}] \\ [K^{41}] & [K^{42}] & [K^{43}] & [K^{44}] & [K^{45}] \\ [K^{51}] & [K^{52}] & [K^{53}] & [K^{54}] & [K^{55}] \end{bmatrix} \begin{Bmatrix} \{u\} \\ \{v\} \\ \{w\} \\ \{\phi\} \\ \{\psi\} \end{Bmatrix} \tag{3.37}$$

The next step after the element matrices, is to solve for the unknowns in the global matrix and then apply the boundary conditions. The elements in the Ritz model are included in the appendix.

3.5 BOUNDARY CONDITIONS

This section explains the various boundary conditions that is used to find a particular property.

3.5.1 NEED FOR BOUNDARY CONDITIONS

In order to solve the system of equations specific boundary conditions should be incorporated and the solution for each loading case associated with that boundary condition being considered is determined. The boundary condition can be categorized into two types namely

natural boundary condition (NBC) and essential boundary condition (EBC). One of the boundary conditions is required for every degrees of freedom to make the system of equations to be resolvable. The NBC indicates the known reactions such as applied moments or forces in the nodes. EBC indicates the know displacements such as rotation or translation. To guarantee the stability of the structure and to eliminate rigid body modes the boundary conditions are highly required. Unstable structure and rigid body modes does not allow to calculate the unknown displacements.

The boundary conditions can be applied based on three assumptions such as mixed boundary conditions, periodic and prescribed boundary conditions. Reactions or displacements can be applied at the nodes of the bounding surface can be done using mixed boundary condition. Periodic boundary condition assumes that node on the top and right moves in relation to the nodes on the bottom and left respectively. If the displacement is applied to all the boundary nodes it is described as prescribed boundary condition. Zhu et al., (2001)., Ren and Silber -Schmidt., (2007) did numerical analysis and found that periodic boundary conditions gave close results to that of analytical methods. On the other hand, mixed boundary conditions gave results below the analytical results (Guo et al., 1999 and Silva et al., 1995).

3.5.2 AFFINE MOTION

Deflection along the boundaries of a structure for every node was determined using the concept of affine motion which is a prescribed form for displacement along the boundary condition.

The equation for affine motion is as follows (Heyliger and McMeeking, 2001)

$$u_i = \epsilon_{ij} x_j \tag{3.38}$$

This equation helps us to calculate the average stress acting on the foams, for the respective applied boundary conditions by using the reactions produced by the displacements at the respective nodes. From the virtual work statement, the average stress is calculated as

$$\sigma_{ij} = \frac{\sum_{k=1}^{N} F_i^k x_j}{V} \tag{3.39}$$

$$\int_V \sigma_{ij}\, \delta\epsilon_{ij} dv = \sum_{i=1}^{N} F_j^i\, \delta u_j^i \tag{3.40}$$

Where σ_{ij} is the average stress, δ is the variational operator, ϵ_{ij} is the strain, N is the number of nodes considered for the boundary condition, F_j^i is the force obtained for the reaction vector in the j-th direction for the i-th node, u_j^i is the displacement for i-th node in the j-th direction, x_j is the coordinate of the node and V is the volume of the structure, which is obtained by multiplying the length * height* thickness for this case.

3.5.3 BOUNDARY CONDITIONS USED IN THIS RESEARCH

For this research, the boundary condition uses affine motion to impose the strain. A unit displacement in applied in the X3 direction. The strain is arbitrarily set to 0.001. External forces and rotations are zero with all loads on the foams applied using displacements. The displacements u, v, w is then calculated using this strain by equation. For the calculation of electric and magnetic potential, the electric and magnetic fields are applied to the boundary nodes.

3.6 CALCULATION OF PROPERTIES

The section explains the calculations for relative density, elastic modulus, shear modulus and Poisson's ratio, and dielectric constant.

3.6.1 RELATIVE DENSITY

Previous analysis explains most of the researchers have solved the mechanical properties of cellular solids by developing the equations as a function of relative density. It is a vital feature of any cellular solids for elastic property calculations however, relative density is not an elastic property.

In this research, the relative density is calculated by multiplying the length, breadth and thickness of each member. These resulting values of each member are summed up and divided by the volume enclosed by the boundaries of the foam.

3.6.2 EFFECTIVE ELASTIC PROPERTIES

The constitutive law was used to find the elastic modulus, shear modulus and Poisson's ratio. The effective elastic property is found by applying a set of boundary conditions and the finding the forces and the displacements in each unit cells. This is a linear response and so the magnitude will be irrelevant.

The constitutive law that relates the average stress to its strain along with its stiffness tensor is given by

$$\sigma_{ij} = C_{ijkl}\epsilon_{kl} \tag{3.41}$$

The generalized Hooke's law in terms of elastic stiffness tensor can be represented in the matrix form as

$$\begin{Bmatrix}\sigma_1\\ \sigma_2\\ \sigma_3\\ \sigma_4\\ \sigma_5\\ \sigma_6\end{Bmatrix} = \begin{bmatrix}C_{11} & C_{12} & C_{13} & 0 & 0 & C_{16}\\ C_{12} & C_{22} & C_{23} & 0 & 0 & C_{26}\\ C_{13} & C_{23} & C_{33} & 0 & 0 & C_{36}\\ 0 & 0 & 0 & C_{44} & C_{45} & 0\\ 0 & 0 & 0 & C_{54} & C_{55} & 0\\ C_{16} & C_{26} & C_{36} & 0 & 0 & C_{66}\end{bmatrix} \begin{Bmatrix}\epsilon_1\\ \epsilon_2\\ \epsilon_3\\ \epsilon_4\\ \epsilon_5\\ \epsilon_6\end{Bmatrix} \tag{3.42}$$

In the similar manner the strain that relates to the stress is given by the generalized Hook's Law as

$$\epsilon_{ij} = S_{ijkl}\sigma_{kl} \tag{3.43}$$

Here σ_{ij} is the average stress acting on the foam to its strain ϵ_{kl} either with stiffness tensor C_{ijkl} or the compliance S_{ijkl} tensor.

3.6.3 PERMITTIVITY

Permittivity is the measure of amount of resistance encountered when forming an electric field in a medium. In general, it is the amount of charge required to develop a unit of electric flux. It is represented by either ε or μ. However, for the Jack packing under study in this research, the diagonal elements of the tensors are identical, and they have non-zero values. Hence it is sufficient to compute one of the diagonal elements for the purpose of the study.

To compute the effective components, the divergence of the electric displacement can be multiplied by a virtual electrostatic potential and integrated over the control volume of the foam. This result can then be integrated by parts to yield the following equation

$$\int_V \delta\varphi D_{i,i}\, dv = 0 = \int_V -\delta\varphi D_{i,i}\, dv + \oint_s \delta Q D_{i,} n_i\, ds \tag{3.44}$$

Using the relationship between the electrostatic potential and electric field, the definition of electric flux allows this equation to be expressed as

$$\int_V D_i \, \delta E_i \, dv = \oint_s q_{n,} \delta Q \, ds \tag{3.45}$$

By introducing the equivalent of an affine electric field, where the variation I potential is simply equal to the virtual electric field multiplied by the spatial coordinate around the boundary of the control volume, giving

$$\delta\varphi = -\delta E_i X_i$$

Substituting this expression into the volume and surface integrals will gives the following

$$\int_V D_i \, \delta E_i \, dv = -\oint_s q_{n,} \delta E_i dX_i \, ds$$

Equating the two terms, assuming that the quantities do not vary over the volume and factoring out the virtual electric field gives

$$D_i = \frac{\sum Q X_i}{V}$$

Where the summation occurs over all of the boundary nodes of the control volume and Q represents the nodal fluxes at those boundary nodes. Since the electric displacement components of, for example, D_X are related to the electric field by the components of the dielectric tensor, we can use the expression

$$D_X = \varepsilon_{XX} E_X$$

Here E_X is known and D_X has been computed. Using this now we can obtain the effective value of ε_{XX}.

3.6.4 EFFECTIVE ELECTRIC AND MAGNETIC PROPERTIES

Piere Curie (1894) was the first person to speculate the Magneto -Electric effect and the Peter Debye (1926) coined this term. However, there is not many researches that explains the concept of piezoelectric and piezo magnetic effects and the boundary conditions used to find them. Hence for this research a boundary condition that is in correlation with the boundary conditions used for effective elastic properties is assumed and the effective piezoelectric and piezomagnetic coefficients for the foams were calculated. For example, to find piezoelectric coefficient of e_{33} an electric potential was applied on the top nodes and constraints were applied for all the other boundaries so that the solid could move freely in the X_3 direction. To find e_{31} the same steps are followed allowing the foam to move in X_1 direction and restraining it in X_3 direction.

The following equations are used to calculate the strain caused by an applied electric field. Using this the piezoelectric coefficients are figured out.

$$S_{ij} = E_k l_{kij} \tag{3.46}$$

$$e_{mij} = l_{mkl} C_{klij} \tag{3.47}$$

where S_{ij} is the strain component, E_k is the component of electric field, l_{kij} are the piezoelectric strain coefficients, C_{klij} are the components of the elastic stiffness.

For the piezomagnetic coefficient a magnetic potential is applied instead of an electric potential and the same procedure is followed to find the coefficients.

The piezomagnetic coefficient d_{mij} is given by

$$S_{ij} = B_k q_{kij} \tag{3.48}$$

$$d_{mij} = q_{mkl} S_{klij} \tag{3.49}$$

The expressions are the same and B_k is the component of magnetic field, q_{kij} are the piezomagnetic strain coefficients.

3.7 MODELLING OF FOAMS

A computational model was created using a Finite Element program written in FORTRAN to solve for the unknown variables. An input file containing all the known values such as number of nodes, number of elements, coordinates and connectivity array of the nodes, material properties along with the EBC and NBC conditions for the jack packed foam and for different thickness and boundary condition is created and incorporated in such a way the code reads this file.

Our complete foam consists of 1331 nodes. For each thickness the code is modified in such a way that the code takes the corresponding nodes for the thickness assumed from the input file. Using this input file, the code will calculate the data required for properties such as half band width, elasticity, electric and magnetic constants. The code is compatible in such a manner that it builds the element matrices and arrange them in the global matrix and for each node, it will calculate all the required variables as per the given boundary conditions before jumping over to the other node. By doing this the processing time is reduced significantly.

CHAPTER 4

RESULTS AND DISCUSSIONS

All the results that are calculated from code are discussed in this chapter. Few parameters are compared with the existing results from Gibson and Ashby (1997) and the behavior is explained and discussed. Results are obtained for the foams with t/l ratio ranging between 0.2 to 1.0 for the jack packed foam structure is tabulated. The entire analysis is purely in three dimensional.

4.1 RELATIVE DENSITY

The relative density of the foam was given according to the equation 3.6.1.1 from chapter 3 with C_1, the numerical constants which depends on the details of cell shape equal to unity. In general, this value ranges between 1 and 4.61 (De Hoff and Rhines, 1966). The values of relative density obtained in this research can be found in table 4.1.

Table 4.1: Relative density $\frac{\rho^*}{\rho_s}$ for the jack packed foam structure

$\frac{t}{l}$	$\frac{\rho^*}{\rho_s}$
0.2	0.104
0.4	0.352
0.6	0.648
0.8	0.896
1.0	1.0

4.2 EFFECTIVE ELASTIC PROPERTIES FOR ISOTROPIC FOAM

In order to validate the computational procedure that has been used in this research, it is important to calculate the elastic properties by using the components of compliance and stiffness tensors before calculating the electric and magnetic properties.

The effective Young's modulus E*/Es is calculated, and a graph is been plotted between the relative density. Table 4.2 gives the values of effective Young's modulus and Effective Poisson's ratio obtained for different t/l ratios of the jack packed foam structure. For the open cell foams, Gibson and Ashby (1997) found a linear relationship between the relative density and the second moment of area of the structure. It is related as

$$\frac{E^*}{E_S} = \left(\frac{\rho^*}{\rho_s}\right)^2 \tag{4.1}$$

Table 4.2: Elastic Properties of Jack Packed Foam. E and G in (10^9 N/m^2), ν^* is dimensionless

t/l	ν	E_s	$\frac{\rho^*}{\rho_s}$	$\frac{E^*}{E_s}$	ν^*
0.2	0.1	2.2	0.104	0.052	0.042
0.4			0.352	0.234	0.071
0.6			0.648	0.557	0.087
0.8			0.896	0.881	0.097
1.0			1.0	1.0	0.1
0.2	0.2	2.4	0.104	0.0512	0.079
0.4			0.352	0.235	0.1282
0.6			0.648	0.556	0.169
0.8			0.896	0.881	0.194
1.0			1.0	1.0	0.2
0.2	0.3	2.6	0.104	0.052	0.1233
0.4			0.352	0.237	0.1901
0.6			0.648	0.557	0.2531
0.8			0.896	0.882	0.2939
1.0			1.0	1.0	0.3
0.2	0.4	2.8	0.104	0.053	0.1848
0.4			0.352	0.243	0.2621
0.6			0.648	0.565	0.341
0.8			0.896	0.885	0.3937
1.0			1.0	1.0	0.4

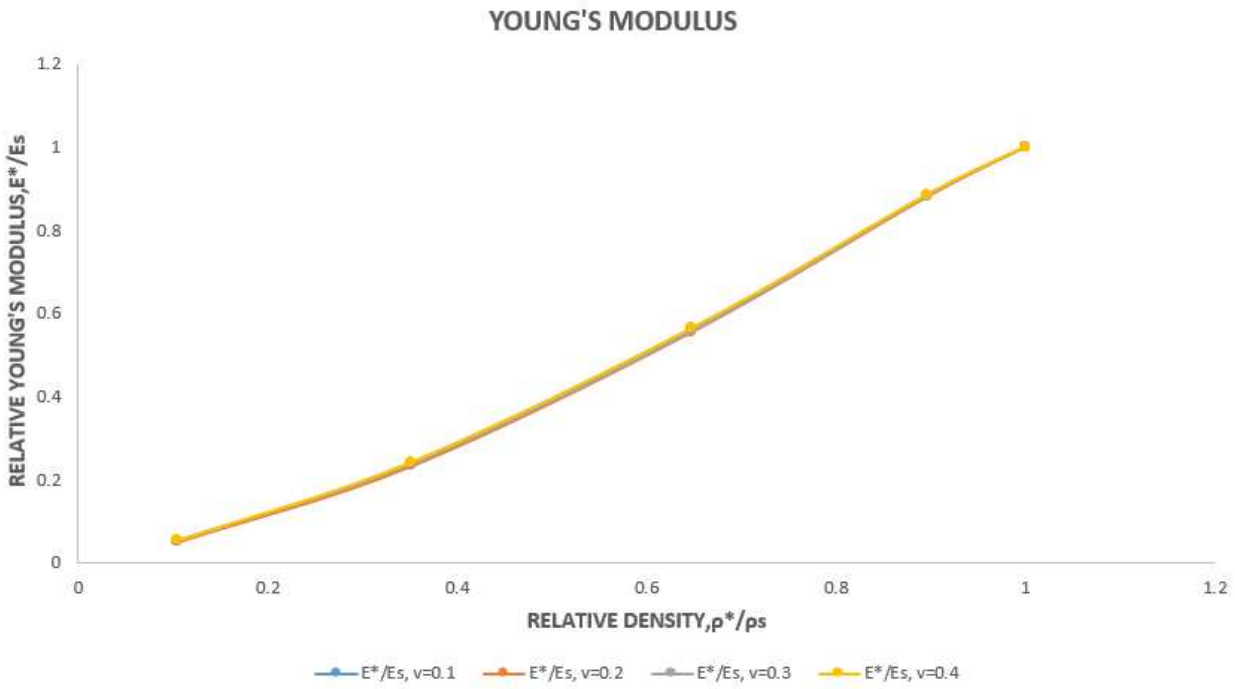

Figure 4.1: Data for the relative Young's modulus of foam plotted against relative density at various Poisson's ratio

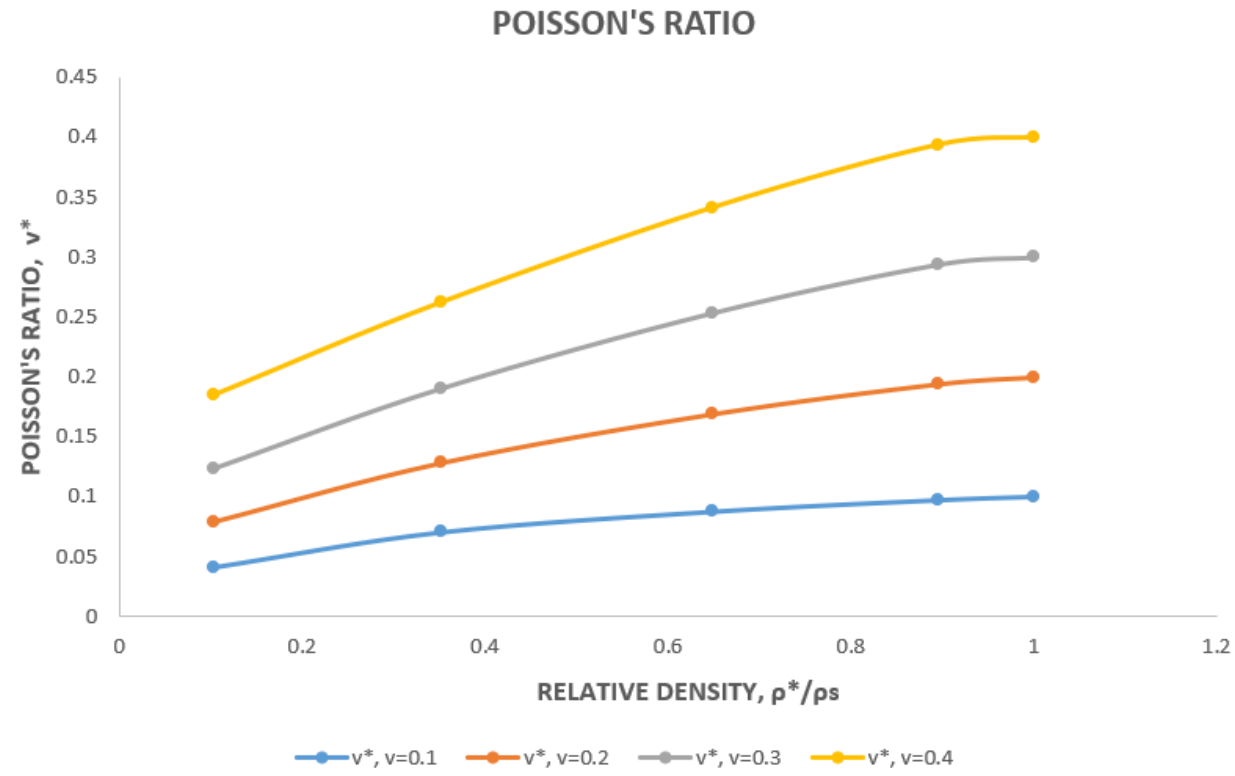

Figure 4.2: Data for Poisson's ratio of the foams plotted against the relative density

The obtained values from the analysis for effective elastic properties of the jack packed foam is used to find the ratio (E^*/E_s) and ν^* and plotted against the relative density for each t/l ratios. The effective Young's Modulus and the effective Poisson's ratio can be found in figure 4.1 and 4.2 respectively.

It is observed from figure 4.1 and 4.2 that the effective Young's modulus of the foam has a linear behavior irrespective of the foam thickness and the effective Poisson's ratio obtained for the foam increases with increase in the thickness and also increases with the increase in the value of Poisson's ratio. This shows that the cell walls of the unit cell experience either tension or compression and there is zero bending during the deformations of the cell walls.

Table 4.3: Effective shear modulus G* for the jack packed foam

t/l	ν	E_s	$\frac{\rho^*}{\rho_s}$	G*
0.2	0.1	2.2	0.104	0.0232
0.4			0.352	0.1993
0.6			0.648	0.5403
0.8			0.896	0.879
1.0			1.0	1.0
0.2	0.2	2.4	0.104	0.0248
0.4			0.352	0.2059
0.6			0.648	0.5459
0.8			0.896	0.8794
1.0			1.0	1.0
0.2	0.3	2.6	0.104	0.0271
0.4			0.352	0.2415
0.6			0.648	0.5534
0.8			0.896	0.8802
1.0			1.0	1.0
0.2	0.4	2.8	0.104	0.0309
0.4			0.352	0.2272
0.6			0.648	0.5643
0.8			0.896	0.8818
1.0			1.0	1.0

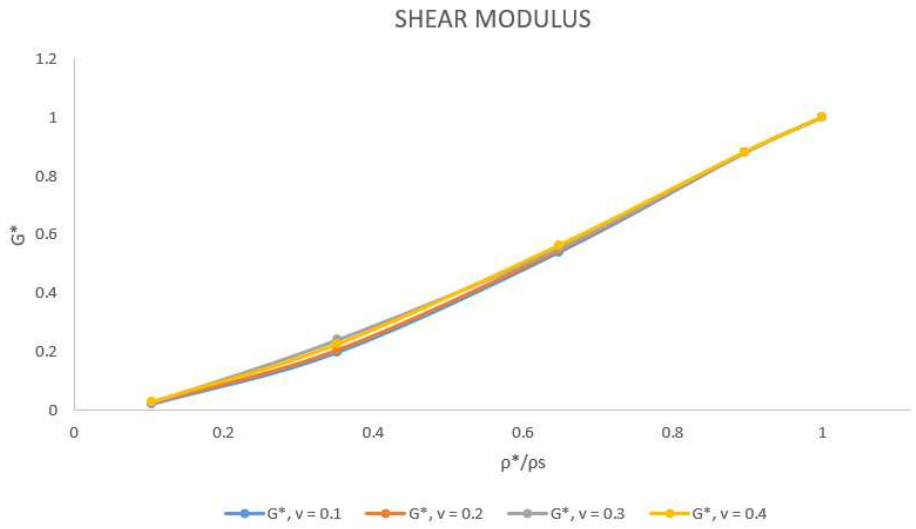

Figure 4.3: Data for shear modulus of the foams plotted against the relative density

Table 4.3 gives the values obtained for effective shear modulus of the jack packed foam at different cell thickness. Figure 4.3 shows the effective shear modulus curve obtained by the analysis and plotted versus the relative density. It is seen from figure 4.3, the curve behaves linearly in the same fashion as that of Young's modulus and increases with increase in the relative densities of the foams at various t/l ratios.

Table 4.4: Permittivity for the jack packed foam

t/l	ν	E_s	$\frac{\rho^*}{\rho_s}$	μ
0.2	0.3	2.6	0.104	0.055
0.4			0.352	0.26
0.6			0.648	0.5853
0.8			0.896	0.8861
1.0			1.0	1.0

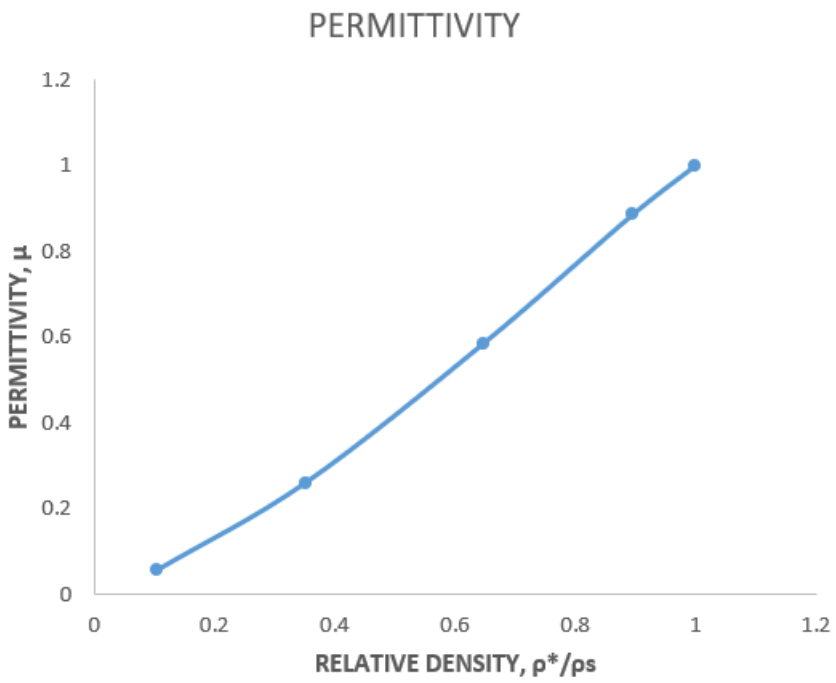

Figure 4.4: Data for permittivity of the foams plotted against the relative density

In general, for the foam modelled in this research the mechanical properties that are considered behaves linearly and increases with increase in the relative density. Also, it is observed that the values merge when the entire thickness is considered for all the considered properties.

4.3 EFFECTIVE PIEZOELECTRIC PROPERTIES

For all the t/l ratio the effective piezoelectric coefficients were calculated using the equation 3.47. It is seen from figure 4.5 for e_{31} , e_{13} , e_{23} , e_{32} the piezoelectric coefficients exhibits a linear behavior with a negative value and turns into a negative exponential value with the increase in relative density and from figure 4.6 that the coefficients of piezoelectricity gives a positive curve for e_{11} , e_{22} , e_{33}.

The obtained piezoelectric coefficients are tabulated in table 4.5 and 4.6.

Table 4.5: Effective Piezoelectric Coefficient for the jack packed foam structure in (C/m^2)

t/l	$\frac{\rho^*}{\rho_s}$	e_{31}
0.2	0.104	-1.625
0.4	0.352	-1.896
0.6	0.648	-2.167
0.8	0.896	-2.438
1.0	1.0	-2.709

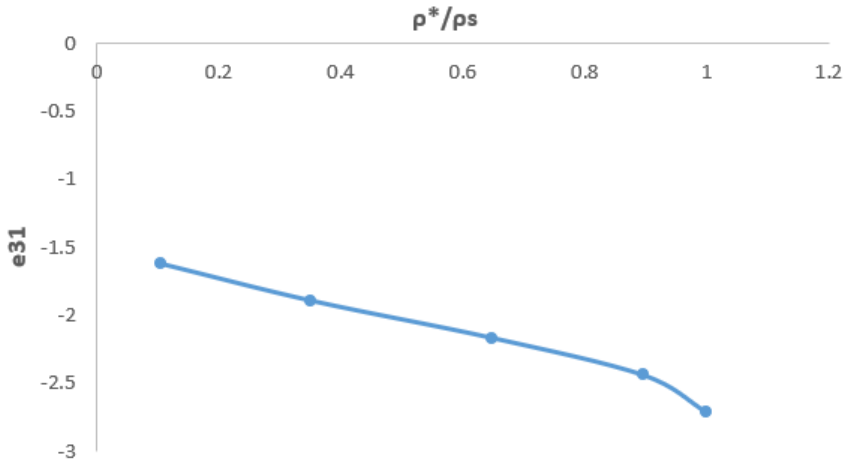

Figure 4.5: Effective piezoelectric coefficient e_{31} for the foam investigated

Table 4.6: Effective Piezoelectric Coefficient for the jack packed foam structure in (C/m^2)

t/l	$\frac{\rho^*}{\rho_s}$	e_{33}
0.2	0.104	5.316
0.4	0.352	6.202
0.6	0.648	7.087
0.8	0.896	7.973
1.0	1.0	8.859

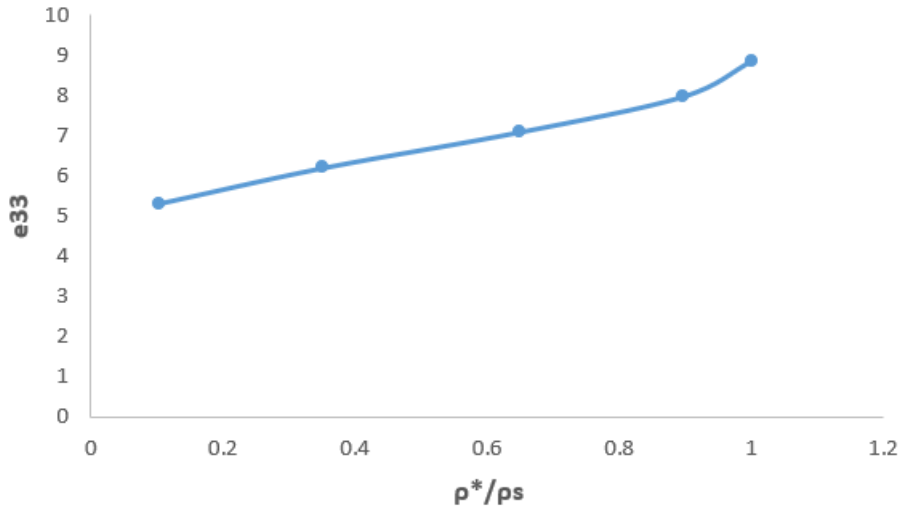

Figure 4.6: Effective piezoelectric coefficient e_{33} for the foam investigated

CHAPTER 5

CONCLUSIONS AND FUTURE WORK

5.1 CONCLUSIONS

Accurately modelling of the foams is required in order to use them effectively in light weight sandwich panels, electronics industry, impact absorbers and other practical applications. A computational model of three-dimensional cellular foam has been studied using finite element analysis to find the mechanical properties of the foams under various boundary conditions and at varying thickness. This thesis has thoroughly investigated the effective elastic, piezoelectric and piezomagnetic properties. The cellular solid is made from Magneto-Electro-Elastic (MEE) material**.**

From the results obtained for the three-dimensional cellular foams, it is concluded that the developed computational model for this research accurately matches the theoretical values and equations. This good correlation with the accepted results for the cellular foams proves that the analysis method is appropriate. The primary conclusion of this research is

1. For the effective Young's modulus, the curve obtained was almost linear with increase in the thickness of the foam with values almost similar to each other.
2. The effective Poisson's ratio increased with increase in thickness as well as for different Poisson's ratio. However, the curve obtained was not linear and it showed a pattern similar to a saturation curve where the curve becomes almost flat with increase in relative density,
3. The shear modulus and the permittivity increase linearly with increase in relative density.

4. For the effective piezoelectric coefficients, the curve obtained shows that the curve starts with a linear behavior but with increase in the relative density the curve gradually becomes into an exponential curve.

5.2 FUTURE WORK

This research presents a solid background for modelling a three-dimensional cellular foam to which any contributions can be added to specific aspects of the structures of the foam.

1. For the same model, the effective pyroelectric and pyro magnetic properties can be explored.
2. Other shapes with varying relative densities can be investigated. A totally different behavior may be obtained due to the shape effect.
3. Cellular irregularities such as cell wall thickness variations, missing cells, closed cells etc. can be investigated. However, the homogenization and the use of RUE will not be used in this case. This in turn may provide a new set of equations.
4. Negative Poisson's ratio should be explored and cross check the properties due to auxetic behavior of the foams resulting from negative Poisson's ratio.
5. As these foams are used in various industries, the effect of free vibrations and dynamic loading must be investigated.
6. Brittle strength, buckling and post elastic behavior of the foams can be researched in the future.
7. Condition such as time dependent variables can be included in the future research work.

BIBLIOGRAPHY

1. Aboudi, J., 2001. Micromechanical Analysis of Fully Coupled Multiphase Composites. *Smart Materials and Structure*, vol 10, pp 867-877.

2. Akbarzadeh, A.M., 2013. Multiphysics of Multilayered and Functionally Graded Cylinders Under Prescribed Hygrothermomagnetoelectromechanical Loading. *Journal of Applied Mechanics*, vol 81, no 4, p 041018.

3. Christensen, R.M., 1986. Mechanics of Low Density Materials. *Journal of the Mechanics and Physics of Solids*, vol 34, pp 563-578.

4. Dunn, M.L., Taya, M., 1993. Electromechanical Properties of Porous Piezoelectric Ceramics. *Journal of American Ceramic Society*, vol 76, no 7, pp 1697-1706.

5. Gan, Y.X., Chen, C., Shen, Y.P., 2005.Three-Dimensional Modelling of the Mechanical Property of Linearly Elastic Open Cell Foams. *International Journal of Solids and Structures*, vol 42, pp 6628-6642.

6. Gent, A.N., Thomas, A.G., 1959. The Deformation of Foamed Elastic Materials. *Journal of Applied Polymer Science*, vol 1, pp 107-113.

7. Gibson, L.J., Ashby, M.F., 1982. The Mechanics of Three-Dimensional Cellular Materials. *Proceedings of the Royal Society of London*, vol A-382, pp 43-59.

8. Gibson, L.J., Ashby, M.F., 1997. *Cellular Solids: Structure and Properties*, 2nd Edition. Cambridge University Press, Cambridge, UK.

9. Gong, L., Kyriakides, S., Traintafyllidis, N., 2005. On the Stability of Kelvin Cell Foams Under Compressive Loads. *Journal of the Mechanics and Physics of Solids*, vol 53, pp 771-794.

10. Guo, X.E., Gibson, L.J., 1999. Behaviour of Intact and Damaged Honeycombs: a Finite Element Study. International Journal of Mechanical Sciences, vol 41, pp 85-105.

11. Harshe, G., Dougherty, J.P., Newnham, R.E., 1993. Theoretical Modelling of 3-0/0-3 Magnetoelectric Composites. International Journal of Applied Electromagnetics, pp 161-171.

12. Heyliger, P.R., McMeeeking, R.M., 2001. Cold Plastic Compaction of Powders by a Network Model. *Journal of the Mechanics and Physics of Solids*, vol 49, pp 2031-2054.

13. Huang, G.Y., Wang, B.L., Mai Y.W., 2009. Effective Properties of Magnetoelectroelastic Materials with Aligned Ellipsoidal Voids. *Mechanics Research Communication*, vol 36, no 5, pp 563-572.

14. Iyer, S., Venkatesh, T.A., 2014. Electromechanical Response of (3-0,3-1) Particulate, Fibrous and Porous Piezoelectric Composites with Anisotropic Constituents: A Model Based on the Homogenization Method. *International Journal of Solids and Structures*., vol 51, no 6, pp 1221-1234.

15. Ko, W.L., 1965. Deformations of Foamed Elastomers. *Journal of Cellular Plastics*, vol 1, pp 45-60.

16. Leaderman, J.M., 1971. The Prediction of the Tensile Properties of Flexible Foams. Journal of Applied Polymer Science, vol 15, pp 693-703.

17. Li, K., Goa, X.L., Roy, A.K., 2005. Micromechanical Modelling of Three-Dimensional Open Cell Foams Using the Matrix Method for Spatial Frames. *Composites: Part B*, vol 36, pp 249-269.

18. Maruyama, B., Spowart, J.E., Hooper, D.J., Mullens., H.M., Druma, A.M., Druma, C., Alam, M.K., 2006. A New Technique for Obtaining Three-Dimensional Structures in Pitch-Based Carbon Foams. *Scripta Materialia*, Vol 54, pp 1709-1713.

19. Menges, G., Knipschild, F., 1975. Estimation of the Mechanical Properties for Rigid Polyurethane Foams. *Polymer Engineering and Science*, vol 15, pp 623-627.

20. Menges, G., Knipschild, F., 1982. Stiffness and Strength-Rigid Plastic Foams. *Mechanics of Cellular Plastics*, N.C. Hilyard, ed., Macmillan, New York, pp 27-72.

21. Nan, C., 1994. Product Property Between Thermal Expansion and Piezoelectricity in Piezoelectric Composites Pyroelectricity. *Material Science*, vol 13, pp 1392-1394.

22. Pan, E., 2001. Exact Solution for Simply Supported and Multilayered Magneto-Electro-Elastic Plates. Journal of Applied Mechanics, vol 68, no 4, pp 608.

23. Pan, E., Heyliger, P.R., 2002. Free Vibrations of Simply Supported and Multilayered Magneto-Electro-Elastic Plates. Journal of Sound Vibrations, vol 252, no 3, pp 429-442.

24. Ramirez, F., Heyliger, P.R., 2006. Free Vibration Response of Two-Dimensional Magneto-Electro-Elastic Laminated Plates. Journal of Sound Vibrations, vol 292, no 3-5, pp 626-644.

25. Reddy, J.N., 2006. *An Introduction to the Finite Element Method*, 3rd Edition. McGraw-Hill, Boston.

26. Roberts, A.P., Garboczi, E.J., 2002. Elastic Properties of Model Random Three-Dimensional Open Cell Solids. *Journal of Mechanics and Physics of Solids*, vol 50, pp 33-35.

27. Sihn, S., Roy, A.K., 2004. Modelling and Prediction of Bulk Properties of Open Cell Carbon Foam. *Journal of the Mechanics and Physics of Solids*, vol 52, pp 197-191.

28. Silva, M.J., Hayes, W.C., Gibson, L.J., 1995. The Effects of Non-Periodic Microstructure and Defects on the Compressive Strength of Two-Dimensional Cellular Solids. *International Journal of Mechanical Sciences*, vol 37, no 11, pp 1161-1177.

29. Smittakorn, W., Heyliger, P.R, 2000. A Discrete Layer of Hygrohermopiezoelectric Plates. *Mechanics of Composite Materials and Structures*, vol 7, pp 79-104.

30. Sun, K.H., Kim, Y.Y., 2010. Layout Design Optimization for Magneto-Electro-Elastic Laminate Composites for Maximized Energy Conversion Under Mechanical Loading. *Smart Materials and Structures*, vol 19, no 5, pp 055008.

31. Steadman, J.A., 2009. Modelling the Elastic Properties of Two-Dimensional Cellular Solids. Master's Thesis. Colorado State University, Fort Collins, CO.

32. Van der Burg, M.W., Shulmeister, V., Van der Geissen, E., Marissen, R., 1997. On the Linear Elastic Properties of Regular and Random Open-Cell Foam Models. *Journal of Cellular Plastics*, vol 33, pp 31-54.

33. Van Run, M.J.G., Terrell, D.R., Scholing, J.H., 1974. An in Situ Grown Eutectic Magnetoelectric Composite Material. *Journal of Material Science*, vol 9, no 10, pp 1710-1714.

34. Warren, W.E., Kraynik, A.M., 1988.The Linear Elastic Properties of Open-Cell Foams. *Journal of Applied Mechanics*, vol 55, pp 341-346.

35. Warren, W.E., Kraynik, A.M., 1997. Linear Elastic Behavior of a Low-Density Kelvin Foam with Open Cells. Journal of Applied Mechanics, vol 64, pp 787-794.

36. Zhang, Z., Wang, X., 2015. Effective Multifield Properties of Electro-Magneto-Thermoelastic Composites Estimated by Finite Element Method Approach. *Acta Mechanica Solida Sinica*, vol 28, no 2, pp 145-155.

37. Zhu, H.X., Knott, J.F., Mills, N.J., 1997. Analysis of the Elastic Properties of Open-Cell Foams with Tetrakaidecahedral Cells. *Journal of Mechanics and Physics of Solids*, vol 45, pp 319-343.

APPENDIX A: ELEMENTS MATRIX EQUATIONS OF THE RITZ MODEL

$$K_{i,j,z}^{11} = \int_A \left[C_{11} \frac{\partial N_i^u}{\partial x}\frac{\partial N_j^u}{\partial x} + C_{55} \frac{\partial N_i^u}{\partial z}\frac{\partial N_j^u}{\partial z} + C_{56} \frac{\partial N_i^u}{\partial z}\frac{\partial N_j^u}{\partial y} + C_{56} \frac{\partial N_i^u}{\partial y}\frac{\partial N_j^u}{\partial z} + C_{66} \frac{\partial N_i^u}{\partial y}\frac{\partial N_j^u}{\partial y} \right] dxdydz \quad \text{(A1)}$$

$$K_{i,j,z}^{12} = \int_A \left[C_{12} \frac{\partial N_i^u}{\partial x}\frac{\partial N_j^v}{\partial y} + C_{14} \frac{\partial N_i^u}{\partial x}\frac{\partial N_j^v}{\partial z} + C_{56} \frac{\partial N_i^u}{\partial z}\frac{\partial N_j^v}{\partial x} + C_{66} \frac{\partial N_i^u}{\partial y}\frac{\partial N_j^v}{\partial x} \right] dxdydz \quad \text{(A2)}$$

$$K_{i,j,z}^{13} = \int_A \left[C_{13} \frac{\partial N_i^u}{\partial x}\frac{\partial N_j^w}{\partial z} + C_{14} \frac{\partial N_i^u}{\partial x}\frac{\partial N_j^w}{\partial y} + C_{55} \frac{\partial N_i^u}{\partial z}\frac{\partial N_j^w}{\partial x} + C_{56} \frac{\partial N_i^u}{\partial y}\frac{\partial N_j^w}{\partial x} \right] dxdydz \quad \text{(A3)}$$

$$K_{i,j,z}^{14} = \int_A \left[e_{31} \frac{\partial N_i^u}{\partial x}\frac{\partial N_j^\phi}{\partial z} + e_{15} \frac{\partial N_i^u}{\partial z}\frac{\partial N_j^\phi}{\partial x} \right] dxdydz \quad \text{(A4)}$$

$$K_{i,j,z}^{15} = \int_A \left[q_{31} \frac{\partial N_i^u}{\partial x}\frac{\partial N_j^\psi}{\partial z} + q_{15} \frac{\partial N_i^u}{\partial z}\frac{\partial N_j^\psi}{\partial x} \right] dxdydz \quad \text{(A5)}$$

$$K_{i,j,z}^{22} = \int_A \left[C_{22} \frac{\partial N_i^v}{\partial y}\frac{\partial N_j^v}{\partial y} + C_{24} \frac{\partial N_i^v}{\partial y}\frac{\partial N_j^v}{\partial z} + C_{44} \frac{\partial N_i^v}{\partial z}\frac{\partial N_j^v}{\partial z} + C_{24} \frac{\partial N_i^v}{\partial z}\frac{\partial N_j^v}{\partial y} + C_{66} \frac{\partial N_i^v}{\partial x}\frac{\partial N_j^v}{\partial x} \right] dxdydz \quad \text{(A6)}$$

$$K_{i,j,z}^{23} = \int_A \left[C_{23} \frac{\partial N_i^v}{\partial y}\frac{\partial N_j^v}{\partial z} + C_{24} \frac{\partial N_i^v}{\partial y}\frac{\partial N_j^v}{\partial y} + C_{44} \frac{\partial N_i^v}{\partial z}\frac{\partial N_j^v}{\partial y} + C_{56} \frac{\partial N_i^v}{\partial x}\frac{\partial N_j^v}{\partial x} \right] dxdydz \quad \text{(A7)}$$

$$K_{i,j,z}^{24} = \int_A \left[e_{32} \frac{\partial N_i^v}{\partial y} \frac{\partial N_j^\phi}{\partial z} + e_{15} \frac{\partial N_i^v}{\partial z} \frac{\partial N_j^\phi}{\partial y} \right] dxdydz \tag{A8}$$

$$K_{i,j,z}^{25} = \int_A \left[q_{32} \frac{\partial N_i^v}{\partial y} \frac{\partial N_j^\psi}{\partial z} + q_{15} \frac{\partial N_i^v}{\partial z} \frac{\partial N_j^\psi}{\partial y} \right] dxdydz \tag{A9}$$

$$K_{i,j,z}^{33} = \int_A \left[C_{33} \frac{\partial N_i^w}{\partial z} \frac{\partial N_j^w}{\partial z} + C_{55} \frac{\partial N_i^w}{\partial x} \frac{\partial N_j^w}{\partial x} + C_{44} \frac{\partial N_i^w}{\partial y} \frac{\partial N_j^w}{\partial y} \right] dxdydz \tag{A10}$$

$$K_{i,j,z}^{34} = \int_A \left[e_{33} \frac{\partial N_i^w}{\partial z} \frac{\partial N_j^\phi}{\partial z} + e_{24} \frac{\partial N_i^w}{\partial y} \frac{\partial N_j^\phi}{\partial y} + e_{15} \frac{\partial N_i^w}{\partial x} \frac{\partial N_j^\phi}{\partial x} \right] dxdydz \tag{A11}$$

$$K_{i,j,z}^{35} = \int_A \left[q_{33} \frac{\partial N_i^w}{\partial z} \frac{\partial N_j^\psi}{\partial z} + q_{24} \frac{\partial N_i^w}{\partial y} \frac{\partial N_j^\psi}{\partial y} + q_{15} \frac{\partial N_i^w}{\partial x} \frac{\partial N_j^\psi}{\partial x} \right] dxdydz \tag{A12}$$

$$K_{i,j,z}^{44} = \int_A \left[-\epsilon_{11} \frac{\partial N_i^\phi}{\partial x} \frac{\partial N_j^\phi}{\partial x} - \epsilon_{22} \frac{\partial N_i^\phi}{\partial y} \frac{\partial N_j^\phi}{\partial y} - \epsilon_{33} \frac{\partial N_i^\phi}{\partial z} \frac{\partial N_j^\phi}{\partial z} \right] dxdydz \tag{A13}$$

$$K_{i,j,z}^{55} = \int_A \left[-\mu_{11} \frac{\partial N_i^\psi}{\partial x} \frac{\partial N_j^\psi}{\partial x} - \mu_{22} \frac{\partial N_i^\psi}{\partial y} \frac{\partial N_j^\psi}{\partial y} - \mu_{33} \frac{\partial N_i^\psi}{\partial z} \frac{\partial N_j^\psi}{\partial z} \right] dxdydz \tag{A14}$$